RNA-sequencing first approach generates new diagnostic candidates in Mendelian disorders.

Carolina Jaramillo Oquendo,[1] Htoo A Wai,[1] Will Rich[1], David J. Bunyan,[2] N. Simon Thomas[2], David Hunt,[1,3], Jenny Lord,[1] Andrew G L Douglas,[1,4] Diana Baralle[1,3*]

1. Human Development and Health, Faculty of Medicine, University of Southampton, Southampton, UK

2. Wessex Genomics Laboratory Service, Salisbury District Hospital, Salisbury, UK

3. Wessex Clinical Genetics Service, University Hospital Southampton NHS Foundation Trust, Southampton, UK

4. Oxford Centre for Genomic Medicine, Oxford University Hospitals NHS Foundation Trust, Oxford, UK

*Correspondence: d.baralle@soton.ac.uk

Abstract

Background: RNA-sequencing is increasingly being used as a complementary tool to DNA sequencing in diagnostics where DNA analysis has been uninformative. RNA-sequencing allows us to identify alternative splicing and aberrant gene expression allowing for improved interpretation of variants of unknown significance (VUS). Additionally, RNA-sequencing provides the opportunity not only to look at the splicing effects of known VUSs but also to scan the transcriptome for abnormal splicing events and expression abnormalities in other relevant genes that may be the cause of a patient's phenotype.

Methods: Using RNA from patient blood, we have systematically assessed transcriptomic profiles of 87 patients with suspected Mendelian disorders, 38% of which did not have a candidate sequence variant. Cases with VUSs and known events were assessed first

1

followed by assessment of cases with no VUS. Each VUS was visually inspected using the

Integrative Genomics Viewer (IGV) to search for splicing abnormalities. Once aberrant

splicing was identified in cases with VUS, multiple open-source alternative splicing tools

(MAJIQ, rMATS-turbo, FRASER2 and LeafCutterMD) were used to investigate if they would

identify what was observed in IGV. Expression outliers were detected using OUTRIDER. To

find diagnoses in cases without a VUS or gene of interest, two separate strategies were used.

The first was a genotype to phenotype approach using variant calls obtained from the RNA-

sequencing and overlapping those calls with results from splicing tools. The second strategy

involved using phenotype information available to filter results from splicing tools.

Results: Using RNA-sequencing only, we were able to assess 71% of VUSs and detect

aberrant splicing in 14/48 patients with a VUS. Furthermore, we identified four new

diagnoses by detecting novel aberrant splicing events in patients with no candidate

sequence variants from prior genomic DNA testing (n=33) or those in which the candidate

VUS did not affect splicing (n=23) and identified one additional diagnosis through detection

of skewed X-inactivation.

Conclusion: We demonstrate the identification of novel diagnoses using an RNA-sequencing

first approach in patients without candidate VUSs. Furthermore, we demonstrate the utility

of blood-based RNA analysis in improving diagnostic yields and highlight optimal approaches

for such analysis.

Keywords

RNA-sequencing, rare disease, diagnostics, splicing, expression,

Background

With the advancement of next generation sequencing, vast amounts of DNA sequencing

data are continually generated to aid in the diagnosis and treatment of rare diseases.

However, our ability to interpret genomic data has not grown at the same rate. The

diagnostic yield of whole exome and genome sequencing alone remains relatively low

leaving scope for diagnostic rates to be improved(1–4). Within the Genomics England

100,000 Genomes Project for example, the average diagnostic yield using whole genome

sequencing is around 25%(3). RNA sequencing (RNA-seq) is now being used as a

complementary tool to DNA sequencing for diagnostic genetic testing in rare disease where

DNA analysis alone has failed to identify a clear diagnosis(5–15). While some studies have

focused on specific disorder types, such as mitochondrial disease(6,12), muscle disorders(5),

and neurodevelopmental disorders(13), others have looked at heterogeneous disease

populations(7,11,14–16). Unlike DNA sequencing, high throughput RNA-seq is both a

qualitative and quantitative approach which allows identification of aberrant splicing (AS),

aberrant gene expression, and mono allelic expression, allowing improved interpretation of

variants of unknown significance (VUSs). An important benefit of the transcriptomic

approach as compared to targeted reverse transcription PCR (RT-PCR) is that it is agnostic to

the resulting abnormally spliced transcript, whereas RT-PCR must rely on targeted primer

designs that are intrinsically limited by factors such as known gene annotations, PCR

amplicon lengths and expected aberrant splicing event. RNA-seq therefore provides the

opportunity not only to look at the splicing effects of known VUSs but also to scan the

transcriptome for abnormal splicing events and expression abnormalities in other relevant

genes that may be the cause of a patient's phenotype. This in turn allows the identification

of molecular diagnoses in patients in which standard genomic DNA testing has not identified

any candidate.

In this study, we have used RNA-seq to a) investigate the feasibility of generating new

diagnostic candidates in a subset of patients with no previously reported candidate VUSs in

3

clinically relevant genes and; b) assess the use of blood as the tissue of choice in the

implementation of an RNA-seq clinical pipeline to improve diagnostic yield of patients with

rare diseases. To understand limitations of available tools we first examined the splicing

effects of clinically relevant VUSs in a heterogeneous cohort of patients with suspected

Mendelian disorders.

Material and Methods

Patient recruitment

Participants were enrolled into the University of Southampton's Splicing and Disease study

with appropriate ethical approval (REC 11/SC/0269, IRAS 49685, ERGO 23056). This cohort

of individuals comprises a combination of rare disease patients assessed by UK clinical

genetics services in whom a candidate VUS may or may not have been identified through

conventional DNA-based testing (n=87). Within this cohort, 48 individuals had pre-existing

candidate VUSs (n=51 variants) that had been previously clinically reported within genes of

potential clinical relevance, six had previously confirmed known genetic diagnoses (4 array

deletions, 1 *PURA* duplication and 1 *PURA* deletion) and 33 had unknown molecular

diagnoses with no previously reported candidate VUSs in clinically relevant genes.

Individuals without molecular diagnosis had a phenotype where a genetic cause was

suspected. 18 of the 51 VUSs have been previously assessed by RT-PCR(10).

Sample collection and RNA extraction

RNA was extracted from 87 blood samples collected in PAXgene blood RNA tubes using the

PAXgene blood RNA Kit (PreAnalytiX, Switzerland). Quantification was performed by

NanoDrop spectrophotometer and Qubit fluorometer (Thermo, MA) and RNA integrity

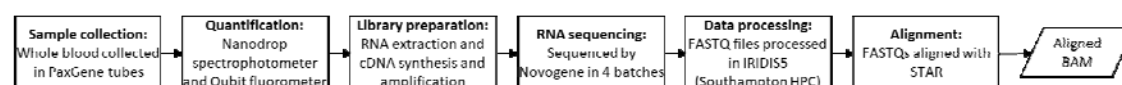number assessed using an Agilent 2100 Bioanalyzer (Agilent, CA).

RNA sequencing

RNA samples were sequenced via Novogene (Hong Kong) in four separate batches

(comprising 7, 16, 33 and 31 samples) using a total RNA-seq approach employing the

NEBNext rRNA Depletion Kit and the NEBNext Ultra Directional RNA Library Prep Kit (New

England Biolabs, MA). Samples in batches 1, 2 and 4 also had NEBNext Globin Depletion Kit

applied, whereas those in batch 3 did not. The library was checked with Qubit and real-time

PCR for quantification and bioanalyzer for size distribution detection. On average 76 million

150 base-pair paired-end reads were generated for each sample on a HiSeq 2000

instrument (Illumina, CA). FASTQ files underwent initial quality control filtering and adapter

sequence removal by Novogene. Filtering included removal of reads containing N>10% (N:

bases that cannot be determined) and reads with over 50% of low quality (Qscore ≤ 5) bases.

Subsequent alignment was performed to the human genome reference (GRCh38) with

annotations from GENCODE(17) release 38 using STAR aligner(18) v2.6.1c with optimised

parameters via the University of Southampton's IRIDIS5 high-performance computing

clusters. Scripts can be found in GitHub

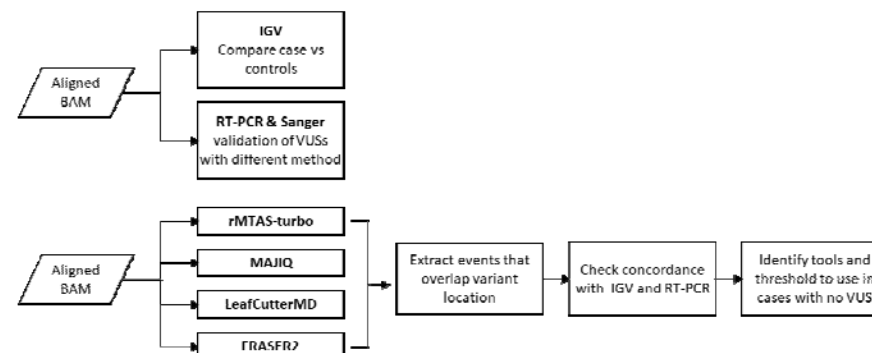[https://github.com/carojoquendo/RNA_splicing_and_disease].

Assessment of aberrant splicing in cases with VUS and known molecular diagnosis

Due to the nature of the cohort, assessment of aberrant splicing and expression was done in

stages. Cases with VUSs and known events were assessed first followed by assessment of
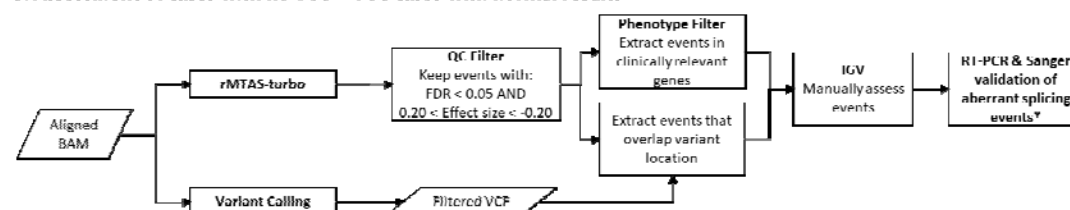
cases with no VUS (**Figure 1**).

Figure 1. *Overview of methods.* **1.** *Data generation. This step was generally the same for all samples (n=87). The only difference came in the library preparation stage where samples in batches 1, 2 and 4 also had globin depletion, whereas samples in batch 3 did not.* **2.** *Cases with a VUS were assessed first. Each variant of unknown significance (VUS) was visually inspected to search for splicing abnormalities in the Integrative Genomics Viewer (IGV). RT-PCR and Sanger sequencing were carried out in parallel for additional validation.* **3.** *Cases without a clinically relevant candidate variant were investigated last. This also included cases for which the original candidate VUS had not been found to alter splicing. Filtering strategy was determined based on observations across cases with a VUS. Results were visualised in IGV, and new diagnostic candidates were validated with RT-PCR and Sanger sequencing.*

To determine the functional consequence at a transcript level for each VUS, RNA-seq data
was loaded into the Integrative Genomics Viewer (IGV)(19) and each variant was visually
inspected to search for splicing abnormalities. If there were no splicing abnormalities in the
exons and introns flanking the variant, it was determined that there were no splicing
abnormalities resulting from the variant. Splicing abnormalities were classed as: exon
skipping, inclusion of cryptic exon, intron retention, alternative 5ꞌ (donor) splice site and
alternative 3ꞌ (acceptor) splice site. The command-line tool ggsashimi(20) was used to
create final sashimi plots to visualise junctions. RT-PCR was carried out in parallel to assess
VUSs where possible. In some cases, RT-PCR was not carried out due to technical limitations
(additional details can be found in the supplemental table 1).

Once aberrant splicing events had been ascertained in cases that had a VUS or known
molecular diagnosis, we used this data to identify open-source tools best placed to identify
potential aberrant splicing in cases for which there was no candidate variant.

FRASER2(21,22), rMATS-turbo v4.1.2(23), MAJIQ v2.4(24) and LeafCutterMD v0.2.9(25)
were used to detect aberrant splicing across all samples. The tools chosen are some of the
most commonly used for splicing analyses, where rMATS-turbo and MAJIQ are events-based
methods while LeafCutterMD and FRASER2 are outlier approaches. We decided to use tools
with two different underlying methodologies as there is still no gold standard for identifying
splicing events in this type of cohort. For all tools except FRASER2, each sample was
compared against other samples within the same batch with the exception of samples in
batch 1 and 2 which were combined to increase power. rMATS-turbo was run with
additional parameters --novelSS to enable detection of novel splice sites, as well as --allow-
clipping to allow alignments with soft or hard clipping to be used. MAJIQ modules build and
DeltaPSI were run with default parameters using the GENCODE v38 annotation gff3 files.

The DeltaPSI results were then input into the MAJIQ voila module which provides a tab-delimited text file to allow parsing of the MAJIQ result and filters out local splice variations (LSVs) with no junctions predicted to change over a certain value. Default parameters for the voila module were used. LeafCutterMD and FRASER2 were also run with default parameters and results were annotated with gene symbols to extract genes and loci of interest for each sample. Once samples had been run through all the tools, events within the gene of interest were extracted to determine if the tools had been able to pick up what had been seen in IGV. This allowed us to check concordance between the tools and identify thresholds that could be used later when looking for events in cases without a VUS.

Assessment of aberrant splicing in patients without candidate VUSs

After cases with VUSs and known events were assessed, we investigated those without a clinically relevant candidate variant. This also included cases for which the original candidate VUS had not been found to alter splicing. The aligned BAM files were run through rMATS-turbo as well as through the GATK's Best Practices workflow for RNA-seq short variant discovery (https://gatk.broadinstitute.org/hc/en-us/articles/360035531192-RNAseq-short-variant-discovery-SNPs-Indels-) to identify variants in the RNA-seq.

Variant calling

First duplicate reads were marked by Picard's version 2.18.14 (http://broadinstitute.github.io/picard) MarkDuplicates function, followed by reformatting of the BAM files for HaplotypeCaller with GATK's (version 4.2.2)(26) SplitNCigarReads and Picard's AddOrReplaceReadGroups. The next step was Base Quality Recalibration, consisting of two tools: GATK's BaseRecalibrator and ApplyBQSR. Lastly GATK's HaplotypeCaller was used to call variants and write to VCF files.

8

To reduce spurious calls, VCF files were run through GATK's VariantFiltration tool, keeping calls with a minimum quality score of 50. bcftools(27) was used to further filter variants excluding any variants with a) less than eight reads covering the locus; b) calls with genotype quality lower than 16; c) calls with strand bias (FS metric) greater than 30; and d) variants with a quality normalised by depth of at least two(28). After filtering, Ensembl's VEP(29) (version 103) was used to annotate the variants with additional information including but not limited to nearest gene, variant consequence (e.g. missense, splice_region) and minor allele frequency (MAF). The SpliceAI VEP plugin was used to produce a score per variant (delta score) based on the likelihood of the variant impacting splicing. SpliceAI scores range from 0-1 with scores closer to 1 being more likely to affect splicing. VCF files were further filtered to keep variants that met all of the following conditions: a) population frequency less than 0.005; b) variants with a SpliceAI score ≥ 0.2; c) variants found in protein coding genes; and d) single nucleotide variants. Indels were not included as the majority had very poor quality and inclusion of indels introduced a significant number of false positives.

Filtering strategies

To find diagnoses in cases without a VUS or gene of interest, two separate strategies were used. The first was a genotype to phenotype approach. Using the annotated and filtered VCF files a BED file was created with variant location, adding 25 base pairs up and downstream of the variant [chromosome start(-25bp) end(+25bp) gene]. rMATS-turbo results were also converted into BED format. After sorting the BED files, the variant BED was overlapped with the rMATS-turbo results BED using bedtools (v2.30)(30) intersect keeping only overlapping features. Each genomic location that was found to overlap a variant and an alternative splicing event identified by rMATS-turbo was then inspected in IGV as previously described.

The second strategy involved using phenotype information available to filter results from

splicing tools. To do this, appropriate panels from the UK Genomic Medicine Service (GMS)

PanelApp(31) resource were applied to the splicing tools results and each AS event was also

inspected in IGV.

Minimum number of sequencing reads & splice effect predictions

The MRSD web portal (https://mcgm-mrsd.github.io/) was used to predict the minimum

number of sequencing reads required from RNA-seq experiments to confidently determine

aberrant splicing events for a gene of interest(32). Default values for confidence level (95%)

and splice junction proportion (75%) were used. For coverage a minimum of five reads were

used (n=5). The online SpliceAI server (https://spliceailookup.broadinstitute.org/) was used

to predict splicing effect of all variants.

RT-PCR and Sanger sequencing

Primers for the variant of interest were designed to span at least three exons and where

possible, up to seven exons. The cDNA was synthesised using High-Capacity cDNA Reverse

Transcription Kit (Thermo Fisher Scientific, USA). PCR was performed using GoTaq G2 DNA

polymerase kit (Promega, USA). The PCR products were analysed in a 1% agarose gel

prepared with Nancy-520 DNA gel stain (Sigma, USA). Subsequently, the PCR products were

purified using the GeneJET PCR Purification Kit (Thermo Fisher Scientific, USA) and

bidirectional Sanger sequencing was carried out by SourceBioscience. PCR experiments

were repeated for reproducibility.

Expression outlier detection

Salmon v1.6.0(36) was used to quantify gene and transcript counts in mapping-based mode.

Transcriptome indices for Salmon were generated using the GRCh38 genome and

transcriptome reference from GENCODE release 38 (https://combine-lab.github.io/alevin-

10

tutorial/2019/selective-alignment/). The R v 4.1.1(37) package tximport v1.22.0(38) was

used to collate and import raw read counts from all samples to be used as input into

OUTRIDER v1.12.0(39). The OUTRIDER function filterExpression was used to remove genes

that had low Fragments Per Kilobase of transcript per Million mapped reads (FPKM)

expression values followed by the OUTRIDER function which ran the full OUTRIDER pipeline.

Results

Summary of RNA-sequencing data outputs

The mean number of sequencing reads per sample was 76.6 million (61.3-130.2 million) and

on average 80% of reads were uniquely mapping (**Figure S1 A & B**). Mean number of splicing

junctions identified across samples (**Figure S1 C**) was 398,718 (303,637-621,161).

Spearman's rank correlation between observed median TPM values and median TPM values

found in the Genotype-Tissue Expression (GTEx) portal(40) was 0.79 with a p-value < 0.001

(**Figure S1 D**) . When considering disease genes from the Online Mendelian Inheritance in

Man (OMIM) database(41) and the UK Genomic Medicine Service's PanelApp resource, 67%

(n=11,128) and 75% (n=2,721) of genes were expressed in blood respectively (TPM >1 in at

least 4 samples).

As mentioned previously, globin depletion was not applied to one of the batches (batch 3).

Analysis of the transcriptomic profiles showed this difference in targeting methodology as

samples within batch 3 clustered together in principal component analysis as well as

hierarchical clustering (**Figure S1 E & F**). Furthermore, median TPM values for the most

abundant haemoglobin genes were in line with values reported in GTEx, which also did not

utilise globin depletion. To avoid bias due to differences in sequencing methodology,

samples were run in separate batches through the splicing tools. TPM values across genes

which had VUSs within our cohort were also assessed (**Figure S2**), which showed that gene

11

coverage in genes of interest was not negatively affected by the lack of globin depletion and

in fact in some cases, the TPM values were higher in batch 3. A possible explanation for the

slight increase of reads in the non-depleted batch is that the globin depletion step could

also be reducing the reads for some non-haemoglobin genes as well(42). A comparison of

the whole transcriptome between batch 3 and the other three batches (**Figure S3**)

demonstrated that globin depletion increased coverage of lower expressed genes (median

TPM 0-1), but in general the lack of globin depletion does not seem to have a large effect on

the transcriptomic profiles.

Splicing analysis in patients with a candidate VUS

We began by looking at the 48 cases which had a VUS to guide our analysis of those for

which we had no candidate variant. This entailed investigation of 51 VUSs across 36

different genes, as some cases had more than one VUS. Using default parameters, the

MRSD tool predicted that we would only be able to assess 47% (n=17) of the 36 genes in

blood based on our mean number of sequencing reads. However, we found this tool to be

overly conservative as we were able to assess 69% of genes (n=25) using RNA-seq alone.

Using the GTEx dataset as a reference(43), median TPM values across the 25 genes ranged

from 0.89 - 73.24 with a mean and median of 19.43 and 11.16 respectively. The

experimental median TPM values in our sequencing data ranged from 2.142 – 75.896 with a

mean and median of 15.718 and 7.637 respectively.

Visual inspection of the RNA-seq BAM files in IGV allowed the detection of aberrant splicing

in 14 cases with candidate VUSs (**Table 1**). Of these splice-altering VUSs, 13/14 were

predicted to affect splicing according to SpliceAI (Δ score ≥ 0.2) and all 14 were validated via

RT-PCR (RT-PCR results for 6 of the 14 variants have been previously reported(44)). The

gene with the lowest median TPM value in GTEx for which we were able to detect aberrant

splicing was *KAT6B* with a GTEx TPM of 0.890 and an experimental median TPM value of

9.79. Out of the 38 VUSs where aberrant splicing events were not detected, 15 variants

could not be assessed as a result of low gene expression in blood (<10 reads covering locus

or normal junctions not observed in sample and controls). For genes where RNA seq was

uninformative, median TPM values according to GTEx ranged from 0.00 to 4.91 with a mean

and median of 0.49 and 0.08 respectively. RT-PCR was able to validate aberrant splicing in

four additional cases with variants in *TERT, PRG4,* and *TAOK1*. Details of all assessed variants

can be found in **Table S1**. Cases (n=23) which showed no aberrant splicing linked to a VUS

were subsequently analysed as unknown cases.

Table 1. Variants of unknown significance (VUSs) for which aberrant splicing (AS) was

observed in IGV. SpliceAI Lookup scores are indicated stating if donor loss (DL), donor gain

(DG), acceptor loss (AL) or acceptor gain (AG) is predicted. Events that were identified by the

splicing tools but had an adjusted p-value > 0.05 are denoted with an asterisk (*).

Gene	Variant of unknown significance (VUS)	SpliceAI prediction (type|Δ score|pre-mRNA pos)	Observed splicing abnormality	Tools that identified aberrant splicing	Median TPM (Experimental |GTEx)
SF3B4	NM_005850.5:c.417C>T Previously reported(10)	DG|0.37|2; AG|0.18|-124	Novel splice donor and acceptor sites in exon 3. r.416_540del, p.(Asp140LeufsTer3)	None	2.142| 46.190
MED13L	NM_015335.4:c.2570-4_2574del Previously reported(10)	AL|0.99|5; AG|0.98|-4	Alternative splice acceptor site in exon 15. r.2570_2578del, p.(Thr857_Asp860delinsAsn)	rMATS, MAJIQ and LeafCutterMD	56.150| 5.887
DKC1	NM_001363.5:c.915+10 G>A Previously reported(10)	DG|0.87|1; DL|0.02|-10	Novel splice donor site in intron 9, r.915_916ins915+1_915+11, p.(Asn307SerfsTer3)	rMATS	7.019| 7.531
NF1	NM_000267.3:c.1168_1179del	DL|0.04|18	Skipping of exon 10 r.1063_1185del,	rMATS	5.981| 1.673

13

Gene	Variant of unknown significance (VUS)	SpliceAI prediction (type|Δ score|pre-mRNA pos)	Observed splicing abnormality	Tools that identified aberrant splicing	Median TPM (Experimental |GTEx)
	Previously reported(10)		p.(Asp355_Lys395del)		
NF1	NM_000267.3:c.7832A>G Previously reported(10)	DG|0.43|-1; AL|0.12|-25; AG|0.01|-83	Skipping of exon 54. r.7870_7970del, p.(Thr2625Ter)	rMATS	5.981| 1.673
P3H1	NM_022356.4:c.1224-80G>A Previously reported(10)	DG|0.62|3	Novel splice acceptor site created within intron 7, r.1223_1224ins1223+1_1223+92, p.(Ser409Ter), r.1223_1224ins1223+1_1223+92, r.1224_1228del, p.(Ser409Ter), r.1223_1224ins1223+1_1223+92, r.1224_1240del, p.(Ser409Ter)	rMATS	3.482| 9.066
TSC2	NM_000548.5:c.4492A>C Previously reported(10)	DL|0.41|1; DG|0.23|-253	Activation of cryptic splice donor site within exon 34, r.4240_4493del, p.(Val1414PhefsTer24)	rMATS and MAJIQ	7.73| 14.030
UBR4	NM_020765.3:c.8488+3A>G	DL|0.26|3; DG|0.13|-117; AG|0.03|430	Retention of intron 57, r. 8488_8489ins8488+1_8489-1, p.(Ser2831ArgfsTer23)	none	15,594| 10.800
SMARCE1	NM_003079.5:c.8-4A>G	AL|0.22|-4; AG|0.48|-1	Alternative 3' splice acceptor site within intron 2, r.7_8ins8-3_8-1 p.(Lys3delinsThrGlu)	none	15.474| 7.107
EFTUD2	NM_004247.4:c.702+5G>A	DL|0.93|5; DG|0.13|-73	Skipping of exon 9, r.620_702del, p.(His208AspfsTer26)	rMATS	17.587| 17.770
ARID1A	NM_006015.6:c.3198G>A	DG|0.25|-65; DL|0.03|0	Skipping of exon 11, r.2989_3198del, p.(Lys997_Gln1066del)	rMATS	7.963| 11.160
KAT6B	NM_012330.4:c.2629+5G>A	DL|0.98|-5; DG|0.02|-37	Skipping of exon 13 r.2536_2629del, p.(Glu846AlafsTer7	rMATS*	9.799| 0.891

Gene	Variant of unknown significance (VUS)	SpliceAI prediction (type|Δ score|pre-mRNA pos)	Observed splicing abnormality	Tools that identified aberrant splicing	Median TPM (Experimental |GTEx)
			1)		
PHF8	NM_015107.3:c.784-2A>G	AL|0.99|-2; AG|0.27|-11	Skipping of exon 8 and skipping of exons 7and 8; r.784_946del, p.(Glu263GlyfsTer6); r.597_946del, p.(Leu200ValfsTer23)	rMATS, MAJIQ and LeafCutterMD	7.536|8.11
WDR26	NM_001379403.1:c.823-10A>G	AG|1.00|-1; AL|0.87|-10	Alternative 3' splice acceptor site in intron 2 (in-frame insertion of three amino acids) r.822_823ins823-9_823-1 p.(Lys274_Ala275insPheLeuGln)	rMATS, MAJIQ and LeafCutterMD	30.680|38.32

The *DKC1* variant (NM_001363.5:c.915+10 G>A) was initially not found to affect splicing

using RT-PCR in our previous publication(44). However, once the effect could be seen using

RNA-seq, it was possible to design targeted assays to confirm the findings on RT-PCR. Thus,

initial detection was not achieved by RT-PCR but post-RNA-seq confirmation was possible.

We ran the RNA seq data through different splicing tools to identify the best tool/s to use

when assessing cases with no candidate variants. The splicing tools rMATS-turbo, MAJIQ,

FRASER2 and LeafCutterMD each identified 11, 4, 4, and 2 of the AS events respectively.

rMATS-turbo had the best sensitivity identifying 79% of the AS events, where 7 were events

identified solely by this tool. The aberrant splicing effects of three variants, *SF3B4* c.417C>T,

UBR4 c.8488+3A>G and *SMARCE1* c.8-4A>G, were consistently missed by all tools. The

SF3B4 variant is predicted to affect splicing (SpliceAI Δ score = 0.37), however, this gene has

a high GC content and low mappability in large regions of its exons. Admittedly, only two

reads mapped to the new junction and there were seven reads with the mutant allele that

did not show aberrant splicing. Nonetheless, this event was validated via RT-PCR [results

previously reported(10)] and has also been characterised using a β-globin hybrid minigene

assay(45). The *UBR4* variant is predicted to cause a donor loss leading to intron retention

(SpliceAI Δ score = 0.26). In IGV 46 reads with the mutant allele and loss of the donor site

were observed, but event was not detected by any of the tools (**Figure S4**). Lastly, the

SMARCE1 variant is predicted to cause an acceptor loss (SpliceAI Δ score = 0.22). Like the

SF3B4 variant, it also has few (n=9) reads mapping to the new junction. All three events

were validated via RT-PCR and in the case of the *UBR4* intron retention with additional qPCR.

Using the evidence from RNAseq and RT-PCR results we were able to identify patterns in the

data that would help us determine potential thresholds and limitations when assessing

cases with no VUSs. This included: 1) SpliceAI predictions showed high concordance

(sensitivity and specificity of 94% and 91% respectively) with the RNAseq and RT-PCR results;

2) In general, for VUSs which caused aberrant splicing, the variant was present in the data

and reads with the mutant allele did not show normal splicing; 3) The splicing tools were

able to detect aberrant events with as low as 5 reads supporting a new junction and; 4)

Intron retention has a higher probability of being missed compared to other aberrant

splicing events.

Splicing analysis in patients without candidate VUSs

The patient cohort without a candidate VUS was comprised of 33 individuals plus an

additional 23 cases where the original candidate VUS had not been found to cause aberrant

splicing. To identify new candidate events in these cases, we took a systematic approach to

narrow down the results obtained from rMATS-turbo to a manageable number so these

could be inspected manually in IGV. rMATS-turbo was the preferred tool as it had the

highest sensitivity identifying aberrant splicing events ascertained in the patients with a VUS.

rMATS-turbo identified an average of 3,578 (2,370-115,522) significant events (FDR < 0.05)

per sample with an inclusion level greater than 0.2 or less than -0.2.

Our first approach used filtered VCF files obtained by the RNA-seq variant calling pipeline to

extract AS events within 25 base pairs of a variant. This first filtering step reduced the mean

number of aberrant splicing events identified ~300 fold to an average of 12 events per

sample. Inspection of all events in IGV led to the identification of two new variants and

associated aberrant splicing events.

Case 1 – S075 (*NARS1*): identification of a splice-altering variant in a child with

undiagnosed global developmental delay. rMATS-turbo identified two AS events within the

NARS1 gene. The first event was an alternative donor site within exon 13 and the second

was retention of intron 13 (**Figure 2**). These events were linked to a heterozygous missense

variant within exon 13 (*NARS1* c.1460C>T) predicted to affect splicing (SpliceAI Δ score =

0.93) by creating a new donor site. Deleterious variants in *NARS1* are associated with

Neurodevelopmental disorder with microcephaly, impaired language, and gait abnormalities,

which would be consistent with the patient's phenotype(46,47). *NARS1* pathogenicity is

generally associated with biallelic deleterious variants, however a recent study by Manole

and colleagues has shown that *de novo* variants, including a recurrent nonsense variant at

the end of the protein can have a gain-of-function effect that alters normal protein function

by interfering with the ATP-binding domain, crucial for enzymatic function(48). In this case

the intron retention is predicted to lead to an out-of-frame transcript, while the new donor

site is predicted to lead to an in-frame deletion of 19 amino acids, both affecting the ATP-
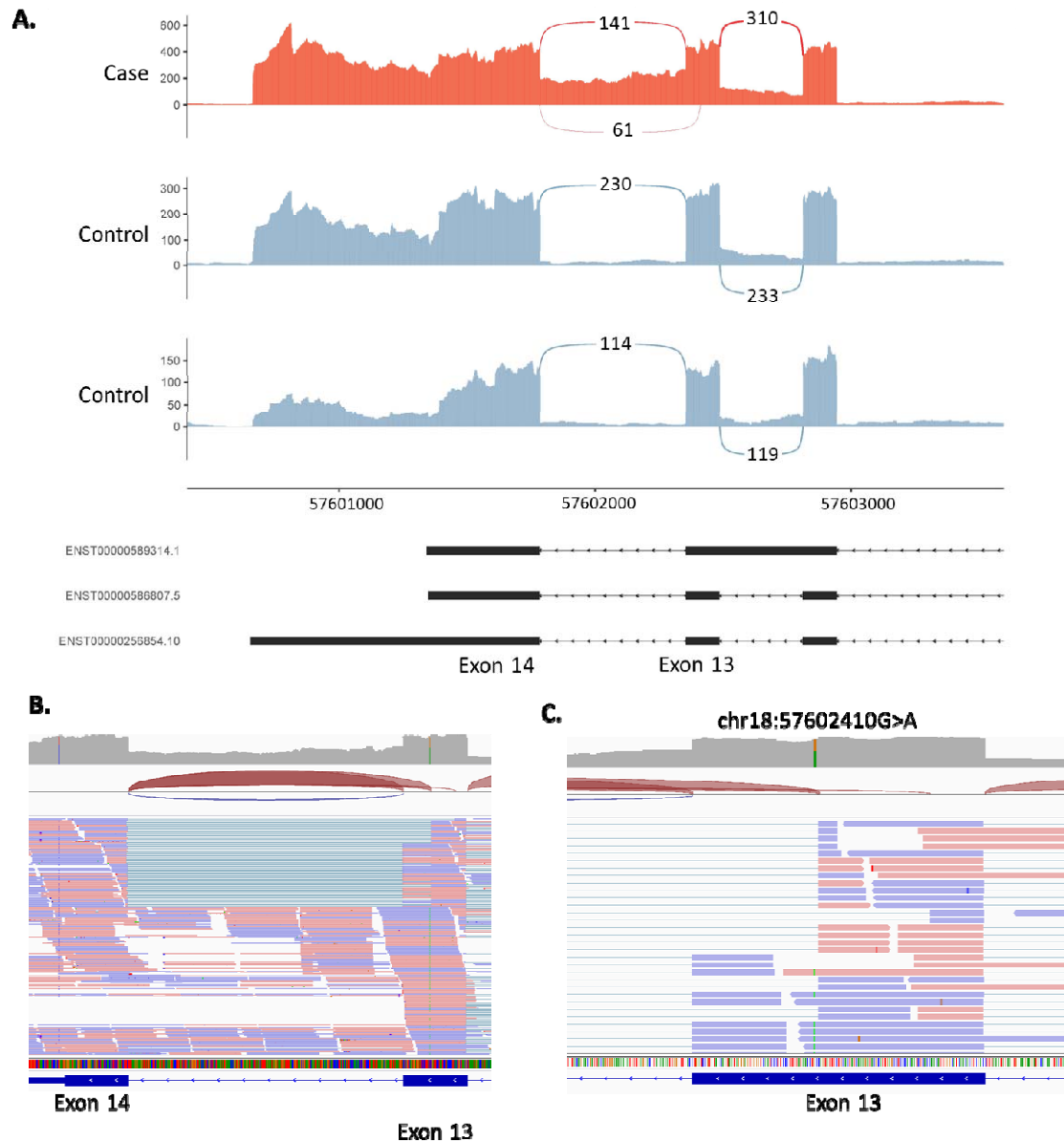
binding domain.

Figure 2. *Alternative donor site and intron retention in NARS1 gene.* *A)* *Sashimi plot of the proband and two controls of the alternative donor and intron retention region in NARS1. For the proband only (red track), we observed an alternative donor site in exon 13 as well as intron 13 retention.* *B)* *IGV screenshot of RNA coverage across exons 13 and 14.* *C)* *Close up of NARS1:c.1460C>T variant, a deep exonic variant predicted to affect splicing by creating a new donor site within exon 13. IGV images all derived from proband RNA-seq data*

Case 2 -S047 (*ARFGEF1*): inclusion of a cryptic exon in a child with undiagnosed

developmental delay. rMATS-turbo identified an AS event within the *ARFGEF1* gene

associated with a deep intronic variant (chr8:67274263A>T,

NM_006421.5:c.1337+1713T>A). This particular case was originally referred for analysis of

a VUS (NM_138927.4:c.1160C>T), which after assessment in IGV was not observed to cause

aberrant splicing. The *ARFGEF1* variant is not predicted to affect splicing (SpliceAI Δ score =

0.0), however, the sequencing data shows the creation of a new acceptor and donor site

within intron 9 suggesting the inclusion of a cryptic exon (**Figure 3**). Inclusion of this cryptic

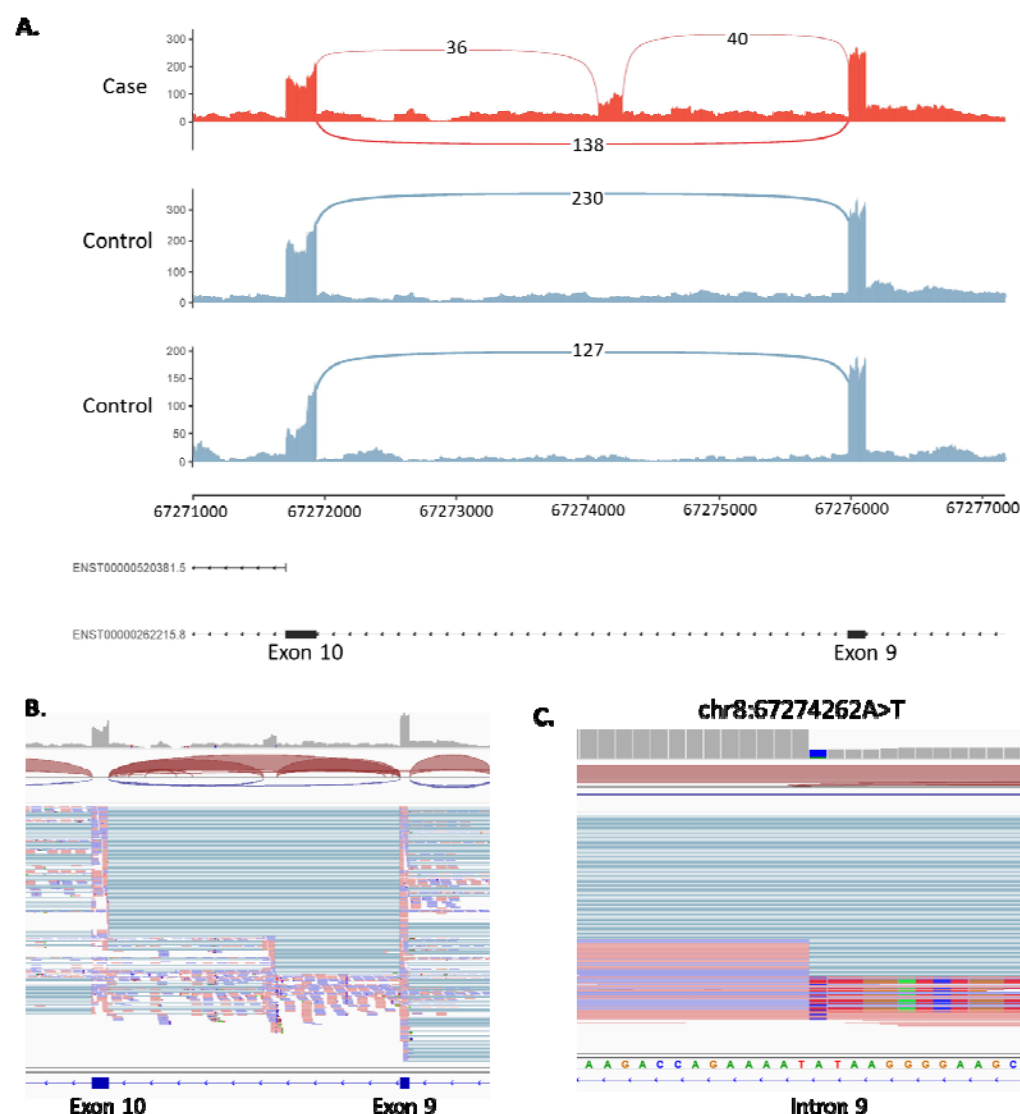exon would result in an out-of-frame insertion of 186 nucleotides p.(Ser447PhefsTer19).

Figure 3. *Activation of cryptic exon caused by intronic variant in ARFGEF1 gene.* *A)* *Sashimi*

plot of the proband and two controls of the ARFGEF1 region of interest. For the proband only

(red track), two novel splice junctions can be seen suggesting the activation of a cryptic exon

in intron 9. *B)* *IGV screenshot of RNA coverage across region of interest.* *C)* *Close up of*

chr8:67274263A>T variant. IIGV images all derived from proband RNA-seq data.

Our second filtering strategy was a phenotype to genotype approach. Using the phenotype

information available, results from the splicing tools were filtered using the appropriate

Genomic Medicine Service (GMS) gene panels. This strategy led to the identification of one

new candidate variant and associated aberrant splicing event.

Case 3 – S076 (*AP4E1*): Identification of cryptic exon inclusion and a second frameshift

variant in a child with undiagnosed hypotonia. The hypotonic infant GMS panel (v18.1) was

applied to rMATS-turbo results, which identified activation of a pseudoexon within intron 1

of *AP4E1* involving use of one alternative splice acceptor site and two alternative donor sites

(**Figure 4**). The two resulting transcripts are predicted to be out of frame, leading to an

insertion of 142 and 38 nucleotides. These events were associated with an intronic variant

(chr15:50911536G>A, NM_007347.5:c.151-542G>A) weakly predicted to affect splicing.

SpliceAI delta scores were 0.11 and 0.09 for acceptor gain (-32bp) and donor gain (5bp)

respectively, but these were just below the 0.2 cut-off. However, analysis of the mutated

sequence using ESEfinder predicts that the G>A base transition identified at this position

may act as an exonic splicing enhancer through the creation of a binding site for splicing

factors SC35 (SRSF2) and/or SRp40 (SRSF5)(49). This event was not picked up by the first

method, as the variant was filtered out due to stringent quality thresholds [genotype quality

(GQ) < 16; variant had a GQ of 6] required to manage noise when calling variants in RNA-seq

data. Considering this gene has a biallelic mode of inheritance, we interrogated the rest of

the gene for a second deleterious event and found a heterozygous single-nucleotide

deletion in exon 6, NM_007347.5:c.567del, p.(Leu190TrpfsTer43), predicted to lead to an

out-of-frame transcript (**Figure 4C**). Further testing confirmed that the variants are

biparental. Biallelic variants in *AP4E1* are associated with spastic paraplegia type 51, which

is consistent with the phenotype information we have available for the proband.
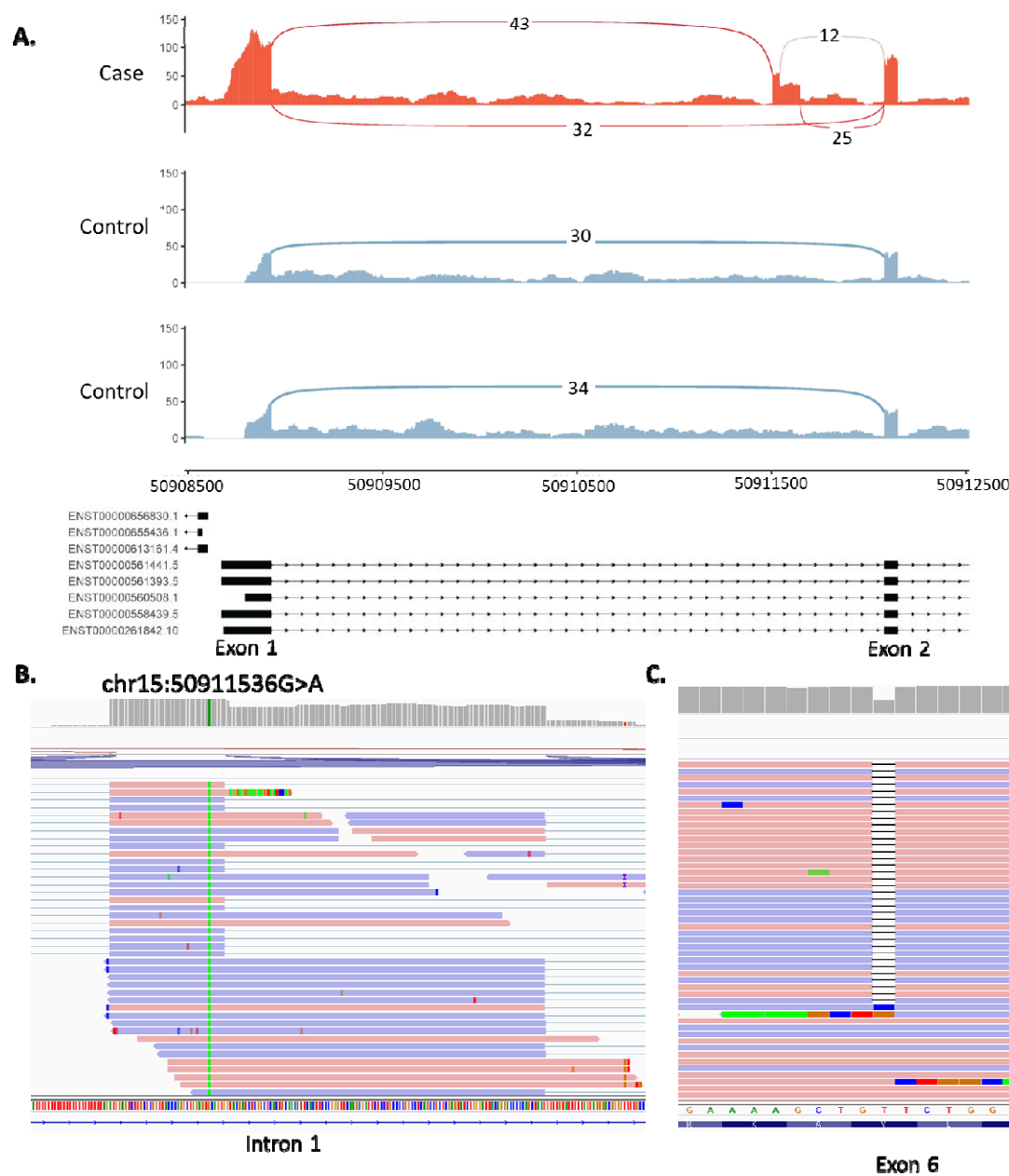
21

Figure 4. *Activation of cryptic exon caused by intronic variant in the AP4E1 gene. **A)** Sashimi plot of the proband and two controls of the AP4E1 region of interest. For the proband only (red track), three novel splice junctions can be seen suggesting the activation of a cryptic exon in intron 1. **B)** Close up of NM_007347.5:c.151-542G>A variant in IGV. **C)** Heterozygous single nucleotide deletion observed in exon 6 (chr15:50929032delT). IGV images all derived from proband RNA-seq data.*

All four variants identified (NM_006421.5:c.1337+1713T>A,

NM_006421.5:c.1337+1713T>A, , NM_007347.5:c.151-542G>A, and NM_007347.5:c.567del)

were Sanger confirmed by the corresponding genetics laboratory subsequently generating

three new diagnostic candidates across these 56 patients.

Gene expression outlier analysis with OUTRIDER

Once aberrant splicing was systematically assessed we investigated if gene expression

profiles would 1) generate new diagnostic candidates and 2) whether expression outliers

correlated with aberrant splicing. OUTRIDER was run across the entire cohort excluding

sample S017 for which only 16% of reads were uniquely mapping (n=86) and identified 175

gene expression outliers (FDR < 0.05) across 39 samples. Of the 39 samples that had

expression outliers 16 were cases with a VUS, 18 were cases without a VUS and 5 were

cases with known molecular diagnosis. Ten cases within our cohort had known chromosome

microdeletions previously identified through microarray analysis (3 cases with known

diagnosis and 7 with unknown diagnosis). In 5/10 of these cases, OUTRIDER identified genes

with significantly lower expression which overlapped the deleted regions previously

identified (**Figure 5**). For the 16 cases which had a VUS, none of the outliers identified

matched the gene in which the VUS was found. A deeper analysis of the results did show

that there were two variants, NM_001363.5(*DKC1*):c.915+10 G>A and

NM_022356.4(*P3H1*):c.1224-80G>A, causing aberrant splicing for which the expression rank

of the gene in which the VUS was found was 1 [lowest expression in the whole cohort] but

was not significant after correction for multiple testing (**Figure S5**). The OUTRIDER gene p-

value before correction was 0.0002 (z-score = -3.76) and 0.0009 (z-score= -3.31) for *DCK1*
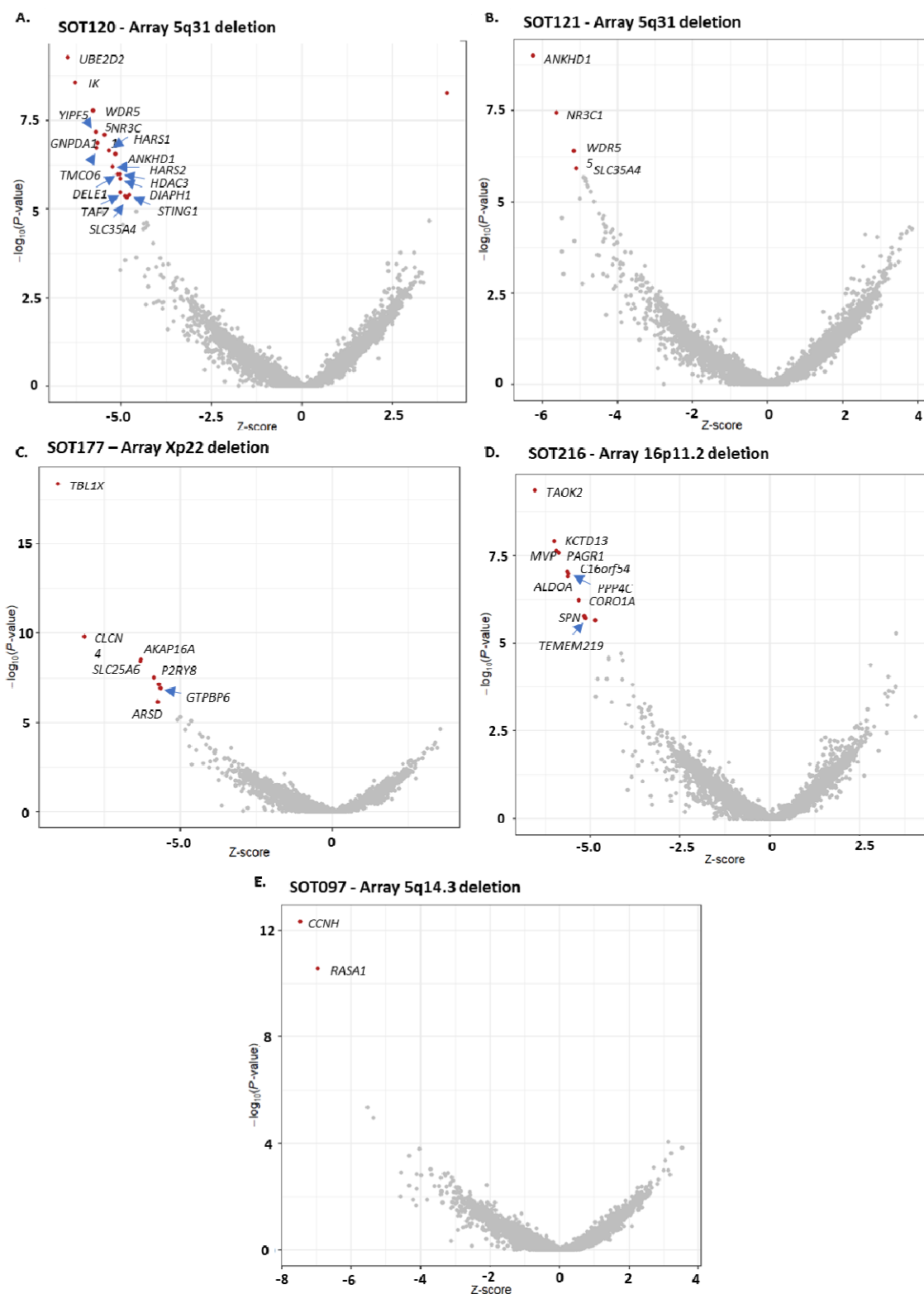
and *P3H1* respectively.

Figure 5. *RNA aberrant expression detection with OUTRIDER.* **A.** *Volcano plot for sample*

SOT120, proband with an array 5q31 deletion. OUTRIDER identified 18 significant gene

*expression outliers (red) of which 17 fell within 5q31. **B.** Volcano plot for sample SOT121,*

proband with an array 5q31 deletion. OUTRIDER identified 4 significant gene expression

*outliers (red) of which 17 fell within 5q31. **C.** Volcano plot for sample SOT177, proband with*

Xp22 deletion. OUTRIDER identified 8 significant gene expression outliers (red) of which 7 fell

*within Xp22. **D.** Volcano plot for sample SOT216, proband with 16p11.2 deletion. OUTRIDER*

identified 11 significant gene expression outliers (red) of which 10 fell within deleted 16p11.2

*region. **E.** Volcano plot for sample SOT097, proband with 5q14.3 deletion. OUTRIDER*

identified 2 significant gene expression outliers (red) both of which fell within the deleted

region.

While gene expression profiles did not generate new diagnostic candidates, OUTRIDER

results did lead to further investigation of one of the analysed cases (SOT177) to confirm

skewed X-inactivation. This individual was a female child with developmental delay and

dysmorphic features. Chromosome microarray analysis had identified a *de novo* 10.2 Mb

deletion of Xp22.33p22.2. However, this copy number variant was classified as a VUS owing

to the child being female and the assumption that the X chromosome carrying the deletion

would be preferentially inactivated. Standard DNA-based X-inactivation testing proved

uninformative in this case, but further primer sets showed unilateral inactivation. Trio

whole-genome sequencing was subsequently undertaken to further seek a potential cause

for the patient's condition. No candidate variant was identified. However, it was possible to

use parental SNP data to determine that the Xp deletion had occurred on the paternal X

chromosome (**Figure S6**). Analysis of 9 additional heterozygous expressed SNPs in the

patient's RNA-seq data from loci across both arms of the X chromosome also revealed

monoallelic paternal expression of X-linked genes (**Figure 6**). This therefore confirms

complete skewing of X-inactivation towards the paternally inherited X-chromosome carrying

the 10.2 Mb deletion. The cause of this extreme skewing currently remains unknown, as no

candidates were found on the maternal X. However, the deletion is now thought to be

causative for the patient's presenting phenotype, resulting in a functional nullisomy for all

genes in the deletion region that are subject to X inactivation.

Locus	Gene	Heterozygous SNPs (GRCh38)	Parental origin	RNA-seq: REF	RNA-seq: ALT	Skewed expression
Xp22.2	MOSPD2	X:14911253:G>A	Maternal	66 reads G	0 reads A	REF 100% - Paternal
Xp22.13	PHKA2	X:18907981:C>T	Maternal	76 reads C	0 reads T	REF 100% - Paternal
Xp11.23	TBC1D25	X:48559322:C>T	Maternal	45 reads C	0 reads T	REF 100% - Paternal
Xp11.22	HUWE1	X:53625883:A>G	Maternal	77 reads A	1 read C (0 reads G)	REF 99% - Paternal
Xq11.2	MTMR8	X:64268644:A>T	Paternal	0 reads A	14 reads T	ALT 100% - Paternal
Xq13.1	PHKA1	X:72695733:G>A	Maternal	6 reads G	1 read A	REF 86% - Paternal
Xq24	DOCK11	X:118605272:A>G	Maternal	201 reads A	0 reads G	REF 100% - Paternal
Xq24	C1GALT1C1	X:120625774:A>T	Paternal	0 reads A	114 reads T	ALT 100% - Paternal
Xq28	IDS	X:149495400:G>A	Paternal	0 reads G	460 reads A	ALT 100% - Paternal

Figure 6. *RNA-seq confirms skewed X-inactivation.* **A.** *IGV screenshots of RNA-seq data from*

WWC3 and CLCN4, which lie within the Xp22.33p22.2 deletion. The patient's sample (top

track) shows no RNA-seq coverage compared to controls. **B.** *IGV screenshots of RNA-seq*

data for heterozygous SNPs illustrating lack of maternal allele expression. **C.** *Table of*

expression of selected heterozygous X-linked SNPs from across the X chromosome confirming

skewing towards the paternal X.

Discussion

In this work we have systematically assessed patients with no candidate VUSs in clinically

relevant genes identifying three new diagnostic candidates and one additional diagnosis

through analysis of expression profiles. We show that it is possible to make diagnoses using

just RNA-seq in patients without a candidate VUS as well as classify VUSs using blood-based

RNA-seq and RT-PCR to uplift diagnostic yield in rare disease patients. This work displays the

variety of events that can be picked up using RNA-seq (i.e. deep intronic and exonic variants,

complex splicing abnormalities, deletions, skewed x-inactivation) highlighting the wide

range of applications this technology can have in the clinical setting.

Splicing analysis in patients with VUSs

High-throughput blood-based RNA sequencing allowed us to evaluate the effect on splicing

of 37/52 VUSs across 48 patients in clinically relevant genes. 38% of assessed VUSs (n=14)

caused aberrant splicing detectable by RNA-seq, helping to clarify variant interpretation and

provide supporting evidence of pathogenicity(50). For the 15/52 VUSs in which splicing

could not be assessed using RNA-seq, the corresponding gene was not expressed in blood.

In comparison to RNA-seq, RT-PCR proved to be more sensitive allowing us to assess 41

VUSs and confirmed a further four likely pathogenic AS events, meaning that in total 35% of

VUSs in this cohort (44% of those that could be adequately assayed) were found to affect

splicing (**see Table S1**). These figures are in concordance with SpliceAI predictions which had

a sensitivity and specificity of 94% and 91% respectively. The increase in sensitivity of RT-

PCR can be attributed to the targeted approach allowing amplification of AS events in lowly

27

expressed genes(51), as well as amplification of AS events with low inclusion levels (in some

cases accounting for NMD). For the nine cases where neither RNA-seq nor RT-PCR was able

to resolve the VUS, such variants would need to be assessed with other tissue types or via

alternative methods such as minigene analysis or potentially using animal models should

the collection of an appropriate or adequately representative tissue not be feasible(51).

The MRSD tool was used to predict the minimum required sequencing depth for genes of

interest and was found to be very conservative. From our empirical data, genes with GTEx

whole-blood TPM values of 5 or above are likely to be assessable for splicing analysis using

the RNA-seq parameters employed in this study, while genes with TPM values down to 0.9

may be assessable by RT-PCR. A TPM threshold of 5 would correspond to 1104/3113 (35%)

of genes listed in the UK Genomic Medicine Service's PanelApp(31) list of disease genes,

while a threshold of 0.9 would include 1866/3113 (60%), see **Figure S7**. Based on our

analysis, we recommend that RT-PCR should be the first-choice test to assess VUSs in genes

with low expression in blood such as *BRCA1, BRCA2* and *FBN1.* In some instances,

informative RT-PCR results can be obtained even in genes reported to have a TPM value of

zero in GTEx(10). However, in most other cases RNA-seq is likely to prove more

advantageous as a first line test. RNA-seq can identify splicing events with more granularity,

particularly when new AS events entail only one or a few nucleotides. Furthermore, with

RNA-seq we can quantify splice isoforms, identify expression outliers, and most importantly

we can look at aberrant splicing events without prior expectation of what the causal

variants may be. Case 4 (SOT247) highlights just how useful having transcriptome wide data

is, as this patient was referred with a VUS that did not cause aberrant splicing, but the

ability to look at the entire transcriptome led to the identification of a likely disruptive

splicing event in a different gene.

While the VUSs in this cohort were enriched for variants affecting splicing, these were

clinically identified VUSs for which clarification of pathogenicity was sought by clinicians,

highlighting the need for this type of tests to be integrated into clinical practice. Overall, we

were able to assess 83% of VUSs (RNA-seq and RT-PCR combined), confirming the utility of

blood as a suitable tissue for validating aberrant splicing in rare disease patients.

Identification of splicing events linked to VUSs by different splicing tools

While we did not set out to benchmark a comprehensive selection of splice junction

detection tools, we did however want to establish if widely used tools could be used to

detect aberrant splicing in rare disease patients as datasets used in previous benchmarking

studies were not comparable to ours(52–54). Using the 14 cases which had aberrant splicing

linked to known VUSs, rMATS-turbo had the highest sensitivity followed by FRASER2, MAJIQ

and then LeafcutterMD. FRASER2 and LeafCutterMD were the two tools developed for

outlier splicing detection and therefore it was unexpected LeafCutterMD had the lowest

sensitivity. There were three variants which were consistently missed by the splicing tools

(*SF3B4* c.417C>T, *UBR4* c.8488+3A>G and *SMARCE1* c.8-4A>G) and is likely that the low

number of reads covering the variants within *SF3B4* and *SMARCE1* is the reason the splicing

tools are not picking up these AS events. We suspect that the low number of reads

supporting the new splicing events are due to nonsense mediated decay or leaky splicing,

however in these two cases, there weren't any coding SNPs to confirm NMD. Long-read may

help with this partially but for short-read data, determining the difference between

partial/leaky splicing and NMD, or possible feedback effects on decreased transcription, will

require new analytical methods. Furthermore, with regards to the intron retention in *UBR4*,

it is unclear why the tools are not identifying this event as there is strong supporting

evidence (**Figure S4**).

Splicing analysis in patients without VUSs

In patients with no prior VUS, the sheer number of significant events resulting from splicing
tools create a challenge in terms of identifying new potential aberrant splicing events that
could be linked to the patients' conditions. However, we were able to filter these down to a
manageable number and identify new likely disruptive aberrant splicing events albeit with
strict filtering criteria, rendering it likely genuine events were missed.

Out of a total of 56 cases without a previously identified VUS or with a VUS but with no
aberrant splicing observed, our RNA-seq analysis identified three cases with relevant
splicing alterations and one case with skewed X-inactivation, suggesting a potential
diagnostic uplift rate of 7%. This is an important untapped group of variants with few
established high-throughput methods of analysis in these types of cohorts(55). We thereby
demonstrate that it is possible to identify new candidate diagnoses and splicing events in
patients with no prior candidate sequence variants, although with a much lower yield than if
a VUS were previously identified. Two of the four new diagnostics candidates were caused
by deep intronic variants, regions of the genome often overlooked in genomic investigations
and where it is difficult to predict functional effects. If prediction algorithms are to be used
for prioritisation of variants, these may need to be tailored by genomic region, such as
having a more permissive SpliceAI score threshold for deep intronic variants. As
demonstrated by the activation of a cryptic exon caused by a deep intronic variant in the
ARFGEF1 gene whose SpliceAI delta score was just below the widely used 0.2 cut-off.

The low diagnostic yield in patients without a candidate VUS could be attributed to a
number of factors: 1) The patient could have a variant affecting splicing in a gene that is not
expressed in blood or there is a tissue specific impact that is not present in blood; 2) The

molecular cause of the disease does not affect splicing; 3) The tools are not able to identify

these events with high confidence (e.g. aberrant isoform is undergoing nonsense mediated

decay or difficult to align) ; 4) Performance of the tools is variable, some events are picked

up better than others (e.g. exon skipping compared to intron retention); and 5) The variant

could have been filtered out.

We were limited to using RNA for variant calling as there was no matching DNA sequencing

available for most cases in this study. Consequently, the high number of false positive

variant calls led to strict filtering criteria where only SNVs were inspected and thus events

caused by indels will have been missed. RNA sequencing may not be ideal for variant calling

as it generates high numbers of false positive calls compared to DNA sequencing due to

both biological and technical differences. Nonetheless, the use of gene panels to restrict

results from the splicing tool (rMATS-turbo) did recover a variant that had been excluded

due to harsh filters. This approach does limit the analysis by restricting to known disease

genes and relies on having robust phenotypic information. If matched whole genome

sequencing data and detailed phenotypic information were available, integration of this

data would likely increase events identified in this patient subgroup and potentially increase

diagnostic yield.

Gene expression analysis

OUTRIDER was able to detect half of the known microdeletions in the cohort, but it did not

detect significant alterations in gene expression in genes which did show aberrant splicing.

There were only two instances where the VUS gene was ranked first (lowest expression for

the whole cohort) and although neither passed the significance threshold, this suggest that

there is a likely decrease of normal transcripts and perhaps decreasing the number of genes

tested (i.e. OMIM or PanelApp genes) could increase the number of significant events

31

identified as well as decreasing the amount of false positives. This finding also indicates that

abnormal splicing is not necessarily associated with a significant reduction in gene

expression, at least in blood, and over-reliance on such expression changes for the

identification of splicing abnormalities is unlikely to have reliable sensitivity. This is

particularly interesting as we would expect many of the splicing abnormalities to shift the

reading frame and therefore undergo nonsense mediated decay (NMD) significantly

decreasing the abundance of the transcript. This lack of change in expression of genes with

aberrant splicing could be a reflection of biological mechanisms indicating that the impact of

NMD is not as effective at depleting aberrant transcripts or it could be due to technical

factors such as limited sensitivity of the tools as mentioned previously; the impact of NMD is

not very pronounced in blood-based RNA-seq and tissue specific RNA-seq is required;

and/or the targeting methodologies bias the type of transcripts and number of transcripts

we observe. Furthermore, whole blood has been shown to have high variability in gene

expression profiles particularly when compared to skin fibroblasts(16). Some studies suggest

that fibroblast RNA enables the investigation of a more comprehensive set of genes than

whole blood and that this is likely the better tissue for detecting clinically relevant

differences in gene expression(12,14,32). While blood-based RNA analysis may not be

optimal, it does offer a number of benefits over fibroblasts. It is more routinely sampled,

less invasive to obtain and does not require cell culture prior to testing, meaning it is faster

to obtain and analyse and has lower requirements in terms of specialised knowledge and

facilities.

Therapeutic applications

Accurate diagnoses facilitate appropriate clinical management, accurate genetic counselling

and informed reproductive decision making, but in some cases, there would be the

32

potential for bespoke RNA-targeted therapies to be designed to correct a given splicing

abnormality and slow or halt the progression of an individual's disease. Cases such as that of

the *AP4E1* cryptic exon inclusion variant highlighted in this study may be especially suitable

targets in this regard, on account of the gradual neurodegenerative nature of the associated

condition and the known efficacy of other antisense oligonucleotide therapies delivered to

the central nervous system such as nusinersen(56,57). Notwithstanding the substantial

challenges and barriers facing development of such bespoke therapeutics, precedent does

exist for n=1 oligonucleotide therapies(58). The utility of RNA-seq in being able to identify

these types of variants means that an effective personalised medicine healthcare system

will benefit from having access to RNA transcriptomics within the diagnostic clinical setting.

Conclusion

To our knowledge, this study is the first to incorporate variant calling data from RNA-seq to

results from splicing tools to identify new diagnostic candidates in rare disease. While the

diagnostic uplift is modest in patients with no known candidate variants in clinically relevant

genes, our analyses suggest at least one third of patients with rare disorders could benefit

from the increased diagnostic yield offered by RNA-seq by providing additional functional

evidence for VUSs. When considering analysis of RNA, RT-PCR should be the first-choice test

to assess VUSs in genes with low expression, but high throughput RNA sequencing is more

advantageous as a first line test. Overall, we were able to validate splicing abnormalities in

35% [18/51] of patients with a VUS and identified four new diagnoses by detecting novel AS

and expression events in patients with no candidate sequence variants, giving an overall

uplift in diagnostic yield of 7% [4/56] in this subset of patients. We believe, that RNA-seq

should be considered as a complementary tool in genetic testing to uplift diagnostic yield in

cohorts of patients with rare disorders particularly when integrated with other omic data.

List of abbreviations

VUS: Variant of unknown significance

IGV: Integrative Genomics Viewer

RNA-seq: RNA sequencing

AS: Aberrant splicing

RT-PCR: Reverse transcription PCR

Declarations

Ethics approval and consent to participate

Participants were enrolled into the University of Southampton's Splicing and Disease study

with appropriate ethical approval (REC 11/SC/0269, IRAS 49685, ERGO 23056).

Consent for publication

Not applicable

Availability of data and materials

The datasets generated and/or analysed during the current study are not publicly available

as ethics approval and consent agreements allow us to share non-identifiable patient data

and analysis data only, as such, we cannot provide BAM or VCF files. The code generated

during this study can be found in GitHub

[https://github.com/carojoquendo/RNA_splicing_and_disease].

Competing interests

The authors declare that they have no competing interests.

Funding

34

Author contributions

Acknowledgements

References

1. Ewans LJ, Minoche AE, Schofield D, Shrestha R, Puttick C, Zhu Y, et al. Whole exome and genome sequencing in mendelian disorders: a diagnostic and health economic analysis. Eur J Hum Genet. 2022 Oct 1;30(10):1121–31.

2. Nurchis MC, Altamura G, Riccardi MT, Radio FC, Chillemi G, Bertini ES, et al. Whole genome sequencing diagnostic yield for paediatric patients with suspected genetic disorders: systematic review, meta-analysis, and GRADE assessment. Arch Public Health. 2023 May 25;81(1):93.

3. 100,000 Genomes Pilot on Rare-Disease Diagnosis in Health Care — Preliminary Report. N Engl J Med. 2021 Nov 11;385(20):1868–80.

4. Álvarez-Mora MI, Sánchez A, Rodríguez-Revenga L, Corominas J, Rabionet R, Puig S, et al. Diagnostic yield of next-generation sequencing in 87 families with neurodevelopmental disorders. Orphanet J Rare Dis. 2022 Feb 19;17(1):60.

5. Cummings BB, Marshall JL, Tukiainen T, Lek M, Donkervoort S, Foley AR, et al. Improving genetic diagnosis in Mendelian disease with transcriptome sequencing. Sci Transl Med. 2017 Apr 19;9(386).

6. Kremer LS, Bader DM, Mertes C, Kopajtich R, Pichler G, Iuso A, et al. Genetic diagnosis of Mendelian disorders via RNA sequencing. Nat Commun. 2017 Jun 12;8:15824.

7. Frésard L, Smail C, Ferraro NM, Teran NA, Li X, Smith KS, et al. Identification of rare-disease genes using blood transcriptome sequencing and large control cohorts. Nat Med. 2019 Jun;25(6):911–9.

8. Gonorazky HD, Naumenko S, Ramani AK, Nelakuditi V, Mashouri P, Wang P, et al. Expanding the Boundaries of RNA Sequencing as a Diagnostic Tool for Rare Mendelian Disease. Am J Hum Genet. 2019 May 2;104(5):1007.

9. Hamanaka K, Miyatake S, Koshimizu E, Tsurusaki Y, Mitsuhashi S, Iwama K, et al. RNA sequencing solved the most common but unrecognized NEB pathogenic variant in Japanese nemaline myopathy. Genet Med Off J Am Coll Med Genet. 2019 Jul;21(7):1629–38.

10. Wai HA, Lord J, Lyon M, Gunning A, Kelly H, Cibin P, et al. Blood RNA analysis can increase clinical diagnostic rate and resolve variants of uncertain significance. Genet Med Off J Am Coll Med Genet. 2020 Jun;22(6):1005–14.

11. Colin E, Duffourd Y, Chevarin M, Tisserant E, Verdez S, Paccaud J, et al. Stepwise use of genomics and transcriptomics technologies increases diagnostic yield in Mendelian disorders. Front Cell Dev Biol [Internet]. 2023;11. Available from: https://www.frontiersin.org/articles/10.3389/fcell.2023.1021920

12. Yépez VA, Gusic M, Kopajtich R, Mertes C, Smith NH, Alston CL, et al. Clinical implementation of RNA sequencing for Mendelian disease diagnostics. Genome Med [Internet]. 2022;14(1). Available from: https://www.scopus.com/inward/record.uri?eid=2-s2.0-85127470335&doi=10.1186%2fs13073-022-01019-9&partnerID=40&md5=2f051e53e887cc2ce85156235eb677e1

13. Dekker J, Schot R, Bongaerts M, Valk WG de, Veghel-Plandsoen MM van, Monfils K, et al. Web-accessible application for identifying pathogenic transcripts with RNA-seq: Increased sensitivity in diagnosis of neurodevelopmental disorders. Am J Hum Genet. 2023;110(2):251–72.

14. Lee H, Huang AY, Wang LK, Yoon AJ, Renteria G, Eskin A, et al. Diagnostic utility of transcriptome sequencing for rare Mendelian diseases. Genet Med Off J Am Coll Med Genet. 2020 Mar;22(3):490–9.

15. Maddirevula S, Kuwahara H, Ewida N, Shamseldin HE, Patel N, Alzahrani F, et al. Analysis of transcript-deleterious variants in Mendelian disorders: implications for RNA-based diagnostics. Genome Biol. 2020 Jun 17;21(1):145.

16. Murdock DR, Dai H, Burrage LC, Rosenfeld JA, Ketkar S, Müller MF, et al. Transcriptome-directed analysis for Mendelian disease diagnosis overcomes limitations of conventional genomic testing [Internet]. Vol. 131, Journal of Clinical Investigation. 2021. Available from: https://www.scopus.com/inward/record.uri?eid=2-s2.0-85098878187&doi=10.1172%2fJCI141500&partnerID=40&md5=5b4afe46dd2a2aa7cd520d169897d88d

17. Frankish A, Carbonell-Sala S, Diekhans M, Jungreis I, Loveland JE, Mudge JM, et al. GENCODE: reference annotation for the human and mouse genomes in 2023. Nucleic Acids Res. 2023 Jan 6;51(D1):D942–9.

18. Dobin A, Davis CA, Schlesinger F, Drenkow J, Zaleski C, Jha S, et al. STAR: ultrafast universal RNA-seq aligner. Bioinforma Oxf Engl. 2013 Jan 1;29(1):15–21.

19. Robinson JT, Thorvaldsdóttir H, Winckler W, Guttman M, Lander ES, Getz G, et al. Integrative genomics viewer. Nat Biotechnol. 2011 Jan;29(1):24–6.

20. Garrido-Martín D, Palumbo E, Guigó R, Breschi A. ggsashimi: Sashimi plot revised for browser- and annotation-independent splicing visualization. PLOS Comput Biol. 2018 Aug;14(8):1–6.

21. Mertes C, Scheller IF, Yépez VA, Çelik MH, Liang Y, Kremer LS, et al. Detection of aberrant splicing events in RNA-seq data using FRASER. Nat Commun. 2021 Jan 22;12(1):529.

22. Scheller IF, Lutz K, Mertes C, Yépez VA, Gagneur J. Improved detection of aberrant splicing using the Intron Jaccard Index [Internet]. medRxiv; 2023 [cited 2023 Nov 3]. p. 2023.03.31.23287997. Available from: https://www.medrxiv.org/content/10.1101/2023.03.31.23287997v1

23. Shen S, Park JW, Lu Z xiang, Lin L, Henry MD, Wu YN, et al. rMATS: robust and flexible detection of differential alternative splicing from replicate RNA-Seq data. Proc Natl Acad Sci U S A. 2014 Dec 23;111(51):E5593-5601.

24. Vaquero-Garcia J, Barrera A, Gazzara MR, González-Vallinas J, Lahens NF, Hogenesch JB, et al. A new view of transcriptome complexity and regulation through the lens of local splicing variations. eLife. 2016 Feb 1;5:e11752.

25. Jenkinson G, Li YI, Basu S, Cousin MA, Oliver GR, Klee EW. LeafCutterMD: an algorithm for outlier splicing detection in rare diseases. Bioinforma Oxf Engl. 2020 Nov 1;36(17):4609–15.

26. Van der Auwera GA, O'Connor BD. Genomics in the Cloud: Using Docker, GATK, and WDL in Terra [Internet]. O'Reilly Media; 2020. Available from: https://books.google.co.uk/books?id=vsXaDwAAQBAJ

27. Danecek P, Bonfield JK, Liddle J, Marshall J, Ohan V, Pollard MO, et al. Twelve years of SAMtools and BCFtools. GigaScience. 2021 Feb 16;10(2).

28. Jehl F, Degalez F, Bernard M, Lecerf F, Lagoutte L, Désert C, et al. RNA-Seq Data for Reliable SNP Detection and Genotype Calling: Interest for Coding Variant Characterization and Cis-Regulation Analysis by Allele-Specific Expression in Livestock Species. Front Genet. 2021;12:655707.

29. McLaren W, Gil L, Hunt SE, Riat HS, Ritchie GRS, Thormann A, et al. The Ensembl Variant Effect Predictor. Genome Biol. 2016 Jun 6;17(1):122.

30. Quinlan AR, Hall IM. BEDTools: a flexible suite of utilities for comparing genomic features. Bioinforma Oxf Engl. 2010 Mar 15;26(6):841–2.

31. Martin AR, Williams E, Foulger RE, Leigh S, Daugherty LC, Niblock O, et al. PanelApp crowdsources expert knowledge to establish consensus diagnostic gene panels. Nat Genet. 2019 Nov;51(11):1560–5.

32. Rowlands CF, Taylor A, Rice G, Whiffin N, Hall HN, Newman WG, et al. MRSD: A quantitative approach for assessing suitability of RNA-seq in the investigation of mis-splicing in Mendelian disease. Am J Hum Genet. 2022;109(2):210–22.

33. Putri GH, Anders S, Pyl PT, Pimanda JE, Zanini F. Analysing high-throughput sequencing data in Python with HTSeq 2.0. Bioinformatics. 2022 May 13;38(10):2943–5.

34. Piovesan A, Caracausi M, Ricci M, Strippoli P, Vitale L, Pelleri MC. Identification of minimal eukaryotic introns through GeneBase, a user-friendly tool for parsing the NCBI Gene databank. DNA Res Int J Rapid Publ Rep Genes Genomes. 2015 Dec;22(6):495–503.

35. Neph S, Kuehn MS, Reynolds AP, Haugen E, Thurman RE, Johnson AK, et al. BEDOPS: high-performance genomic feature operations. Bioinforma Oxf Engl. 2012 Jul 15;28(14):1919–20.

36. Patro R, Duggal G, Love MI, Irizarry RA, Kingsford C. Salmon provides fast and bias-aware quantification of transcript expression. Nat Methods. 2017 Apr;14(4):417–9.

37. R Core Team. R: A language and environment for statistical computing [Internet]. Vienna, Austria: R Foundation for Statistical Computing; 2021. Available from: https://www.R-project.org/

38. Soneson C, Love MI, Robinson MD. Differential analyses for RNA-seq: transcript-level estimates improve gene-level inferences. F1000Research. 2015;4:1521.

39. Brechtmann F, Mertes C, Matusevičiūtė A, Yépez VA, Avsec Ž, Herzog M, et al. OUTRIDER: A Statistical Method for Detecting Aberrantly Expressed Genes in RNA Sequencing Data. Am J Hum Genet. 2018 Dec 6;103(6):907–17.

40. The Genotype-Tissue Expression (GTEx) project. Nat Genet. 2013 Jun;45(6):580–5.

41. Amberger JS, Bocchini CA, Schiettecatte F, Scott AF, Hamosh A. OMIM.org: Online Mendelian Inheritance in Man (OMIM®), an online catalog of human genes and genetic disorders. Nucleic Acids Res. 2015 Jan;43(Database issue):D789-798.

42. Harrington CA, Fei SS, Minnier J, Carbone L, Searles R, Davis BA, et al. RNA-Seq of human whole blood: Evaluation of globin RNA depletion on Ribo-Zero library method. Sci Rep. 2020 Apr 14;10(1):6271.

43. Carithers LJ, Ardlie K, Barcus M, Branton PA, Britton A, Buia SA, et al. A Novel Approach to High-Quality Postmortem Tissue Procurement: The GTEx Project. Biopreservation Biobanking. 2015 Oct;13(5):311–9.

44. Wai HA, Lord J, Lyon M, Gunning A, Kelly H, Cibin P, et al. Blood RNA analysis can increase clinical diagnostic rate and resolve variants of uncertain significance. Genet Med. 2020 Jun 1;22(6):1005–14.

45. Cassina M, Cerqua C, Rossi S, Salviati L, Martini A, Clementi M, et al. A synonymous splicing mutation in the SF3B4 gene segregates in a family with highly variable Nager syndrome. Eur J Hum Genet EJHG. 2017 Feb;25(3):371–5.

46. Wang L, Li Z, Sievert D, Smith DEC, Mendes MI, Chen DY, et al. Loss of NARS1 impairs progenitor proliferation in cortical brain organoids and leads to microcephaly. Nat Commun. 2020 Aug 12;11(1):4038.

47. Manole A, Efthymiou S, O'Connor E, Mendes MI, Jennings M, Maroofian R, et al. De Novo and Bi-allelic Pathogenic Variants in NARS1 Cause Neurodevelopmental Delay Due to Toxic Gain-of-Function and Partial Loss-of-Function Effects. Am J Hum Genet. 2020 Aug 6;107(2):311–24.

48. Manole A, Efthymiou S, O'Connor E, Mendes MI, Jennings M, Maroofian R, et al. De Novo and Bi-allelic Pathogenic Variants in NARS1 Cause Neurodevelopmental Delay Due to Toxic Gain-of-Function and Partial Loss-of-Function Effects. Am J Hum Genet. 2020 Aug 6;107(2):311–24.

49. Cartegni L, Wang J, Zhu Z, Zhang MQ, Krainer AR. ESEfinder: A web resource to identify exonic splicing enhancers. Nucleic Acids Res. 2003 Jul 1;31(13):3568–71.

50. Richards S, Aziz N, Bale S, Bick D, Das S, Gastier-Foster J, et al. Standards and guidelines for the interpretation of sequence variants: a joint consensus recommendation of the American College of Medical Genetics and Genomics and the Association for Molecular Pathology. Genet Med. 2015 May 1;17(5):405–23.

51. Wai HA, Constable M, Drewes C, Davies IC, Svobodova E, Dempsey E, et al. Short amplicon reverse transcription-polymerase chain reaction detects aberrant splicing in genes with low expression in blood missed by ribonucleic acid sequencing analysis for clinical diagnosis. Hum Mutat. 2022 Jul;43(7):963–70.

52. Ding L, Rath E, Bai Y. Comparison of Alternative Splicing Junction Detection Tools Using RNA-Seq Data. Curr Genomics. 2017 Jun;18(3):268–77.

53. Mehmood A, Laiho A, Venäläinen MS, McGlinchey AJ, Wang N, Elo LL. Systematic evaluation of differential splicing tools for RNA-seq studies. Brief Bioinform. 2020 Dec 1;21(6):2052–65.

54. Jiang M, Zhang S, Yin H, Zhuo Z, Meng G. A comprehensive benchmarking of differential splicing tools for RNA-seq analysis at the event level. Brief Bioinform. 2023 Apr 5;bbad121.

55. Marwaha S, Knowles JW, Ashley EA. A guide for the diagnosis of rare and undiagnosed disease: beyond the exome. Genome Med. 2022 Feb 28;14(1):23.

56. Ebrahimi-Fakhari D, Teinert J, Behne R, Wimmer M, D'Amore A, Eberhardt K, et al.
Defining the clinical, molecular and imaging spectrum of adaptor protein complex 4-
associated hereditary spastic paraplegia. Brain. 2020 Oct 1;143(10):2929–44.

57. Pane M, Coratti G, Sansone VA, Messina S, Catteruccia M, Bruno C, et al. Type I spinal
muscular atrophy patients treated with nusinersen: 4-year follow-up of motor,
respiratory and bulbar function. Eur J Neurol. 2023 Mar 7;

58. Kim J, Hu C, Moufawad El Achkar C, Black LE, Douville J, Larson A, et al. Patient-
Customized Oligonucleotide Therapy for a Rare Genetic Disease. N Engl J Med. 2019 Oct
24;381(17):1644–52.

Additional files

Figure S1: PDF: Overview of RNA sequencing data. Additional figure detailing, distribution of

uniquely mapping reads, total number of junctions, correlation of experimental TPM values

versus GTEx values as well as clustering of samples based on transcriptomic profiles.

Figure S2: PDF: Median transcript per million (TPM) values in genes with a variant of

uncertain significance (VUS) across the four batches. Bar plot comparing TPM values across

each batch in genes of interest.

Figure S3: PDF: Effects of globin depletion on gene expression. Figure showing correlation

and comparison of TPM values between globin depleted and non-depleted batches.

Figure S4: PDF: Intron retention caused by intronic variant in *UBR4*. Sashimi plot and RNA-

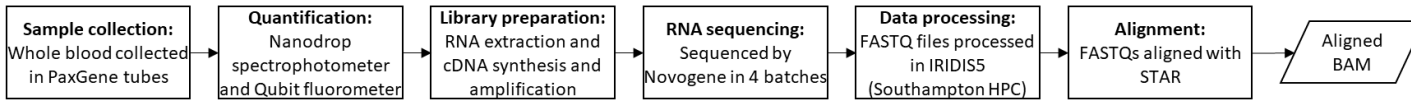seq IGV screenshot of aberrant splicing observed in patient with *UBR4* variant.

Figure S5: PDF: Gene rank plots for *DKC1* and *P3H1*. Dot plot showing OUTRIDER expression

rank for *DKC1* and *P3H1*.

Figure S6: PDF: Trio whole genome sequencing confirms paternal chromosomal origin of a

Xp22.33p22.2 deletion. SNP data within the deleted region of female patient with
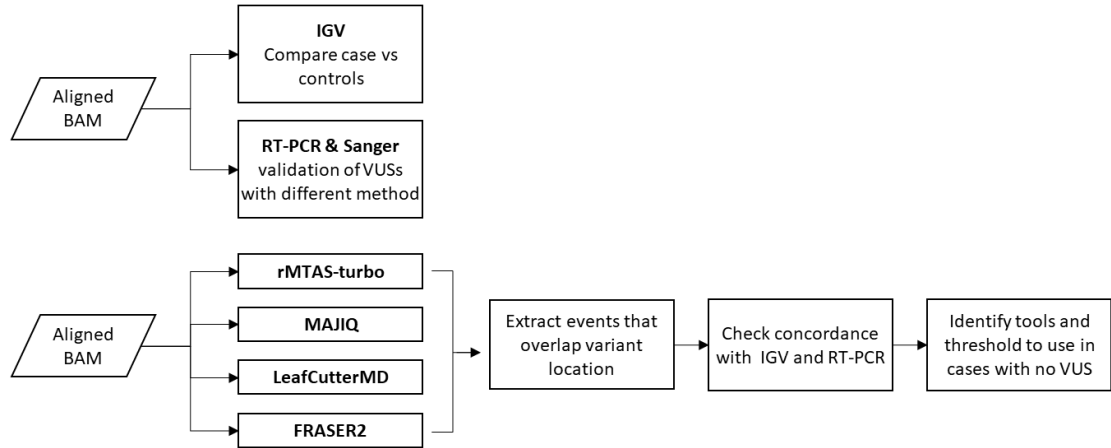
Xp22.33p22.2 deletion of 10.2 Mb.

Figure S7: PDF: GTEx blood TPM values across selected different gene panels available via

the UK Genomic Medicine Service. Breakdown of GTEx blood TPM values for selected panels

available in the UK Genomic Medicine Service.

Table S1: xlsx: Detailed list of samples and variants assessed using RNA-seq and RT-PCR.

1. Data Generation

| Sample collection: Whole blood collected in PaxGene tubes | → | Quantification: Nanodrop spectrophotometer and Qubit fluorometer | → | Library preparation: RNA extraction and cDNA synthesis and amplification | → | RNA sequencing: Sequenced by Novogene in 4 batches | → | Data processing: FASTQ files processed in IRIDIS5 (Southampton HPC) | → | Alignment: FASTQs aligned with STAR | → | Aligned BAM |

2. Assessment of cases with VUS + cases with known events

Aligned BAM →

- **IGV** — Compare case vs controls
- **RT-PCR & Sanger** — validation of VUSs with different method

Aligned BAM →

- **rMTAS-turbo**
- **MAJIQ**
- **LeafCutterMD**
- **FRASER2**

→ Extract events that overlap variant location → Check concordance with IGV and RT-PCR → Identify tools and threshold to use in cases with no VUS

3. Assessment of cases with no VUS + VUS cases with normal results

Aligned BAM →

- **rMTAS-turbo** → **QC Filter** Keep events with: FDR < 0.05 AND 0.20 < Effect size < -0.20 →
  - **Phenotype Filter** Extract events in clinically relevant genes
  - Extract events that overlap variant location
  → **IGV** Manually assess events → **RT-PCR & Sanger validation of aberrant splicing events***
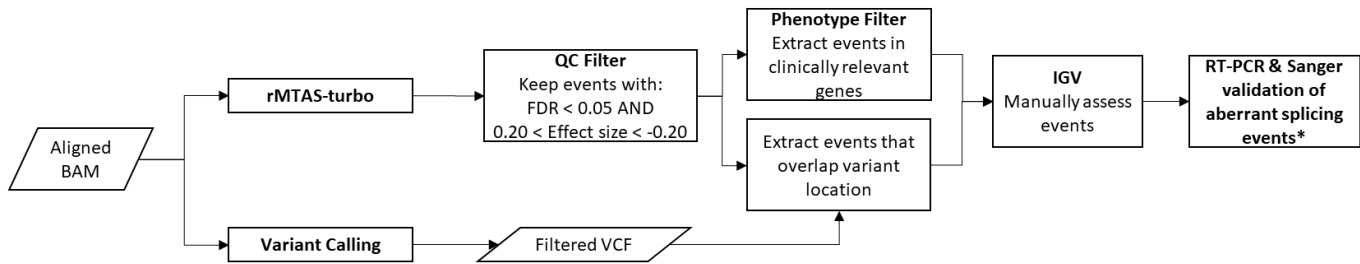- **Variant Calling** → Filtered VCF →

Figure 1. Overview of methods. **1.** Data generation. This step was generally the same for all samples (n=87). The only difference came in the library preparation stage where samples in batches 1, 2 and 4 also had globin depletion, whereas samples in batch 3 did not. **2.** Cases with a VUS were assessed first. Each variant of unknown significance (VUS) was visually inspected to search for splicing abnormalities in the Integrative Genomics Viewer (IGV). RT-PCR and Sanger sequencing were carried out in parallel for additional validation. **3.** Cases without a clinically relevant candidate variant were investigated last. This also included cases for which the original candidate VUS had not been found to alter splicing. Filtering strategy was determined based on observations across cases with a VUS. Results were visualised in IGV, and new diagnostic candidates were validated with RT-PCR and Sanger sequencing.
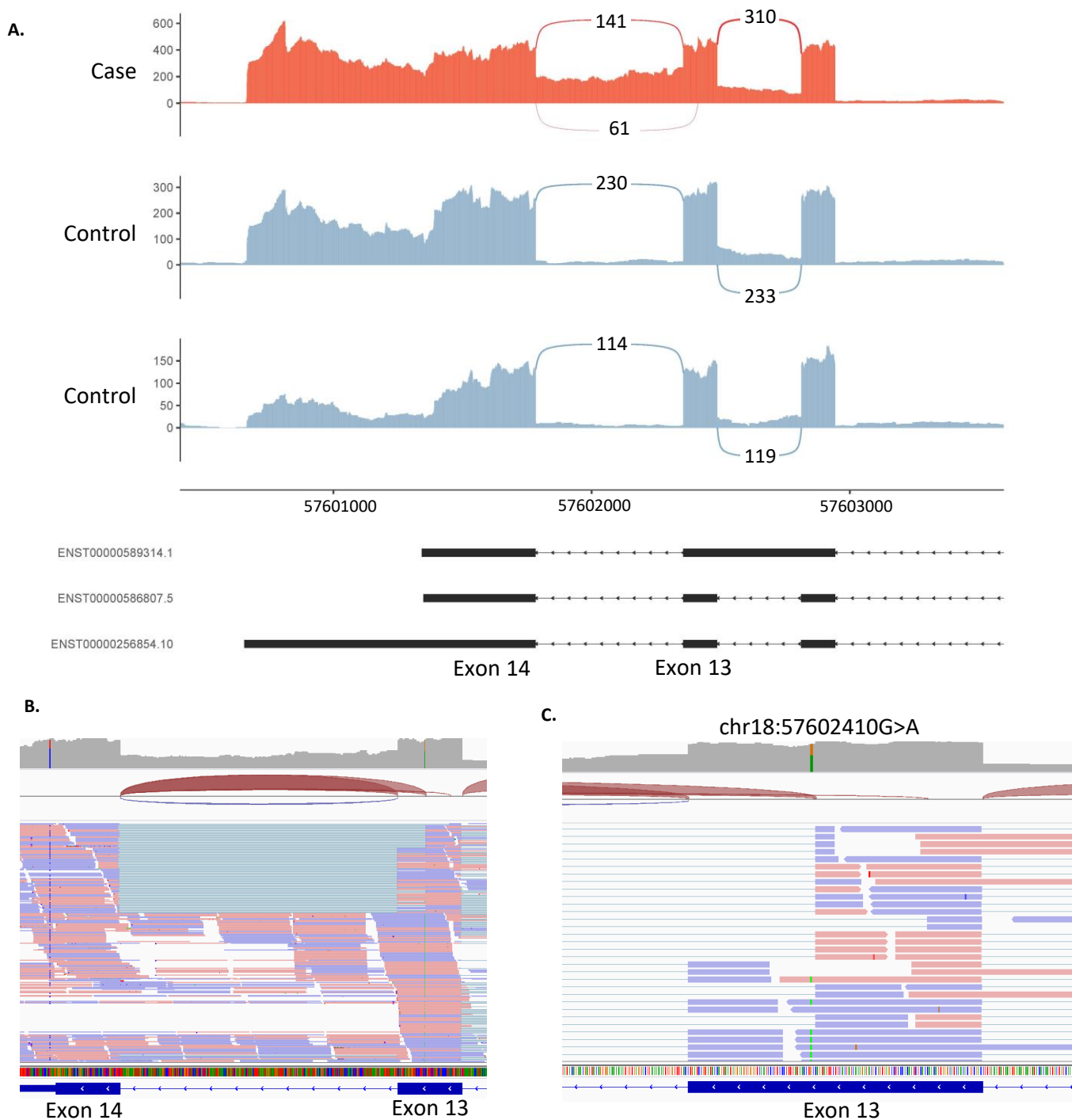
Figure 2. Alternative donor site and intron retention in *NARS1* gene. **A.** Sashimi plot of the proband and two controls of the alternative donor and intron retention region in *NARS1.* For the proband only (red track), we observed an alternative donor site in exon 13 as well as intron 13 retention. **B.** IGV screenshot of coverage across exons 13 and 14. **C.** Close up of *NARS1* c.1460C>T variant, a deep exonic variant predicted to affect splicing by creating a new donor site within exon 13. IGV images all derived from proband RNA-seq data.
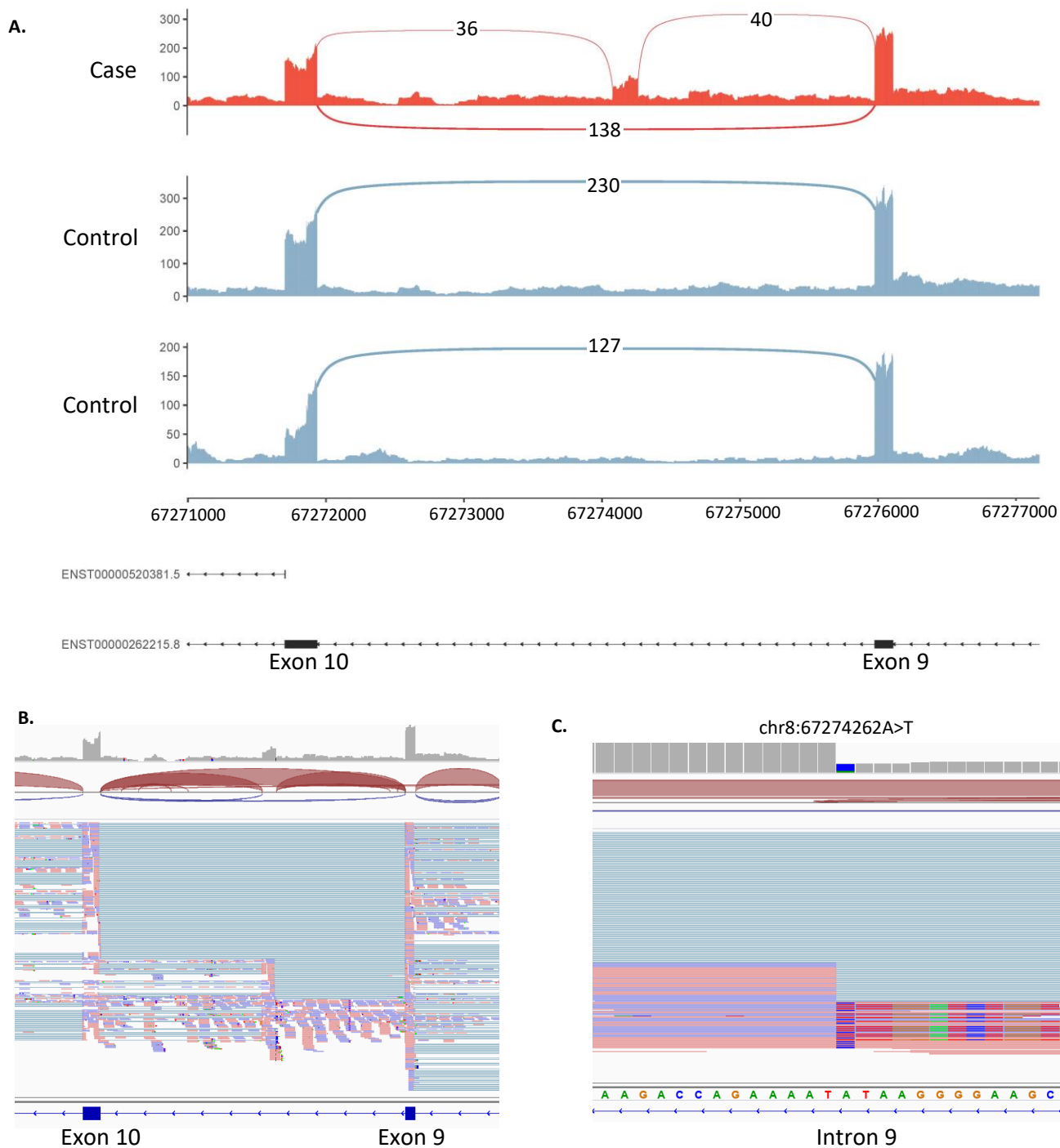
Figure 3. Activation of cryptic exon caused by intronic variant in *ARFGEF14* gene. **A.** Sashimi plot of the proband and two controls of the *ARFGEF14* region of interest. For the proband only (red track), two novel splice junctions can be seen suggesting the activation of a cryptic exon in intron 9. **B.** IGV screenshot of coverage across region of interest. **C.** Close up of chr8:67274262A>T variant. IGV images all derived from proband RNA-seq data.
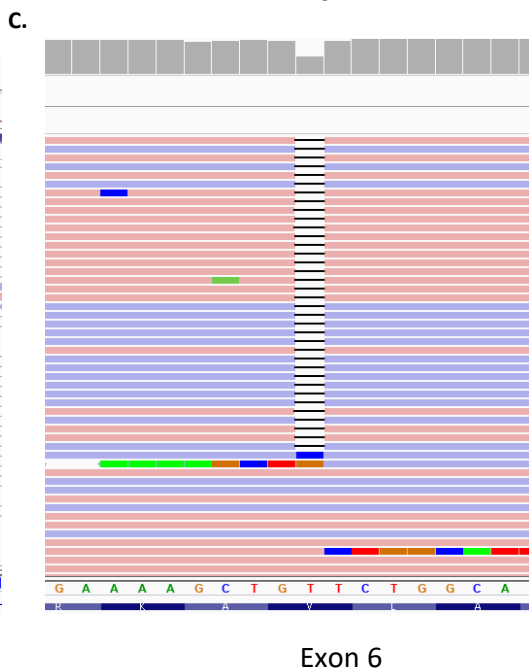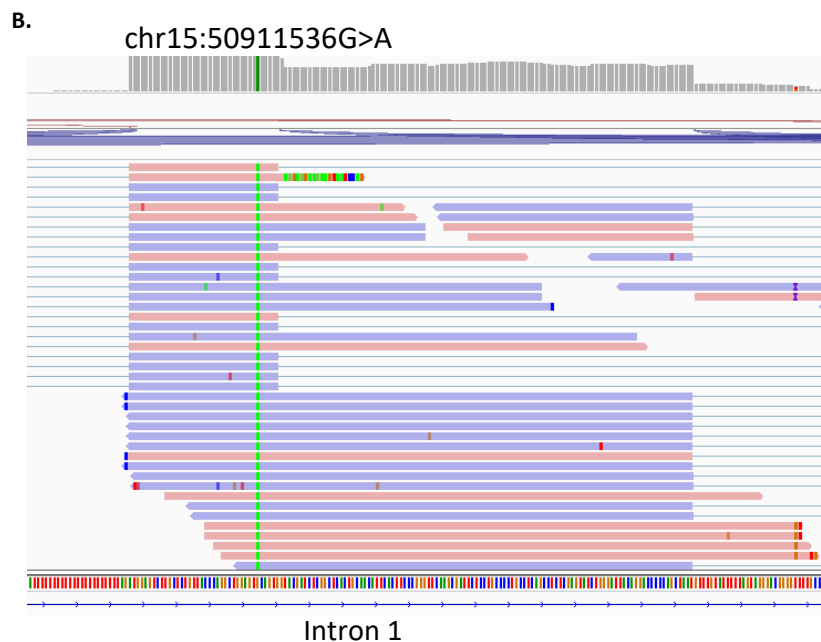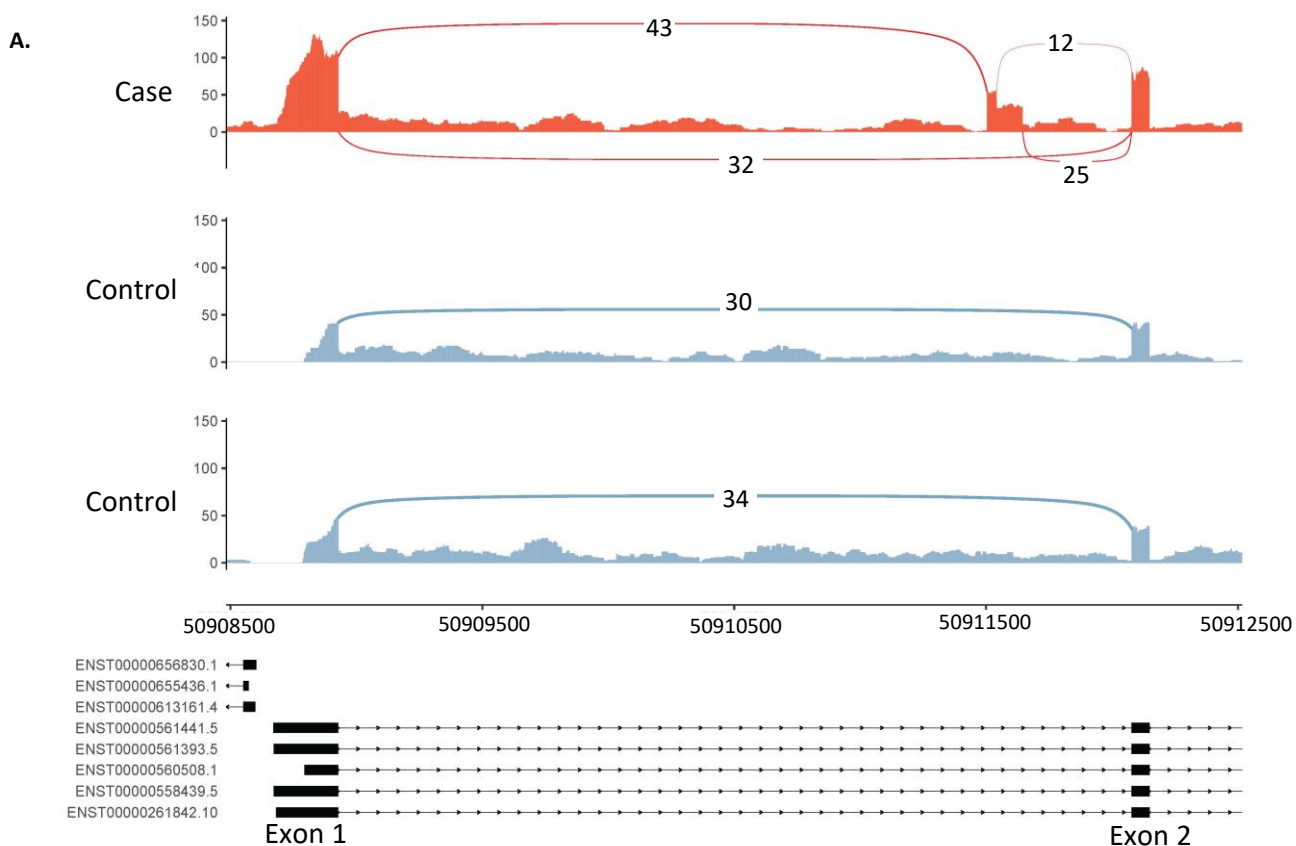
Figure 4. Activation of cryptic exon caused by intronic variant in the *AP4E1* gene. **A.** Sashimi plot of the proband and two controls of the *AP4E1* region of interest. For the proband only (red track), three novel splice junctions can be seen suggesting the activation of a cryptic exon in intron 1. **B.** Close up of NM_007347.5:c.151-542G>A variant in IGV. **C.** Heterozygous single nucleotide deletion observed in exon 6 (chr15:50929032delT). IGV images all derived from proband RNA-seq data.
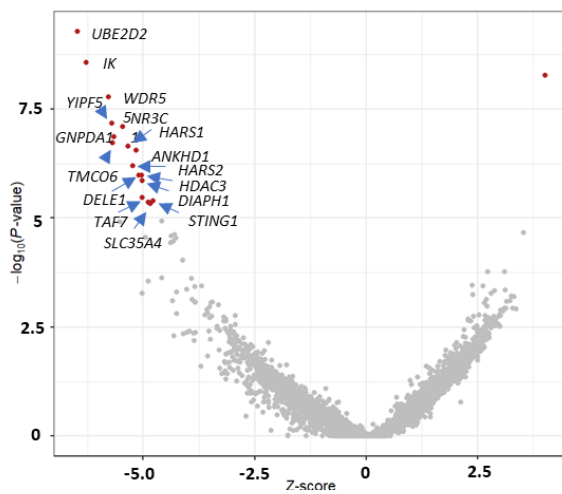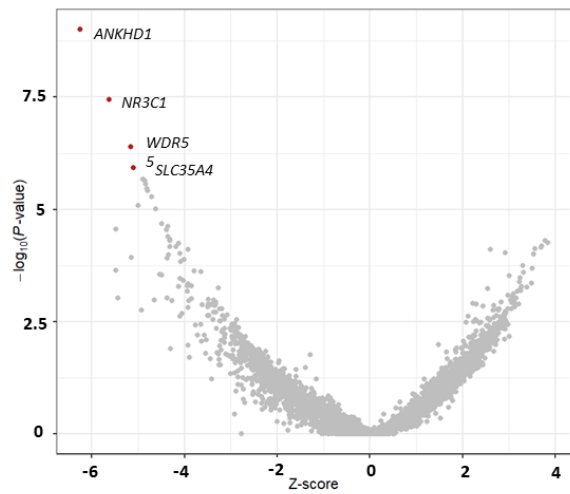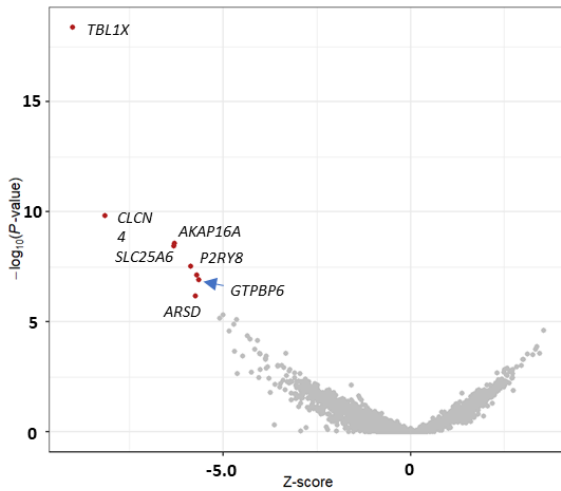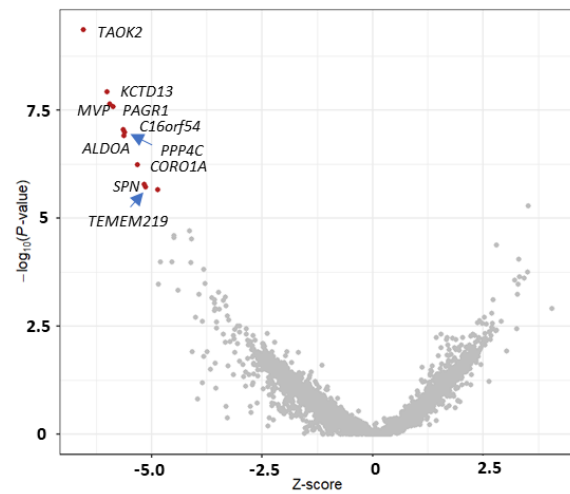
Figure 5. RNA aberrant expression detection with OUTRIDER. **A.** Volcano plot for sample SOT120, proband with an array 5q31 deletion. OUTRIDER identified 18 significant gene expression outliers (red) of which 17 fell within 5q31. **B.** Volcano plot for sample SOT121, proband with an array 5q31 deletion. OUTRIDER identified 4 significant gene expression outliers (red) of which 17 fell within 5q31. **C.** Volcano plot for sample SOT177, proband with Xp22 deletion. OUTRIDER identified 8 significant gene expression outliers (red) of which 7 fell within Xp22. **D.** Volcano plot for sample SOT216, proband with 16p11.2 deletion. OUTRIDER identified 11 significant gene expression outliers (red) of which 10 fell within deleted 16p11.2 region. **E.** Volcano plot for sample SOT097, proband with 5q14.3 deletion. OUTRIDER identified 2 significant gene expression outliers (red) both of which fell within the deleted region.
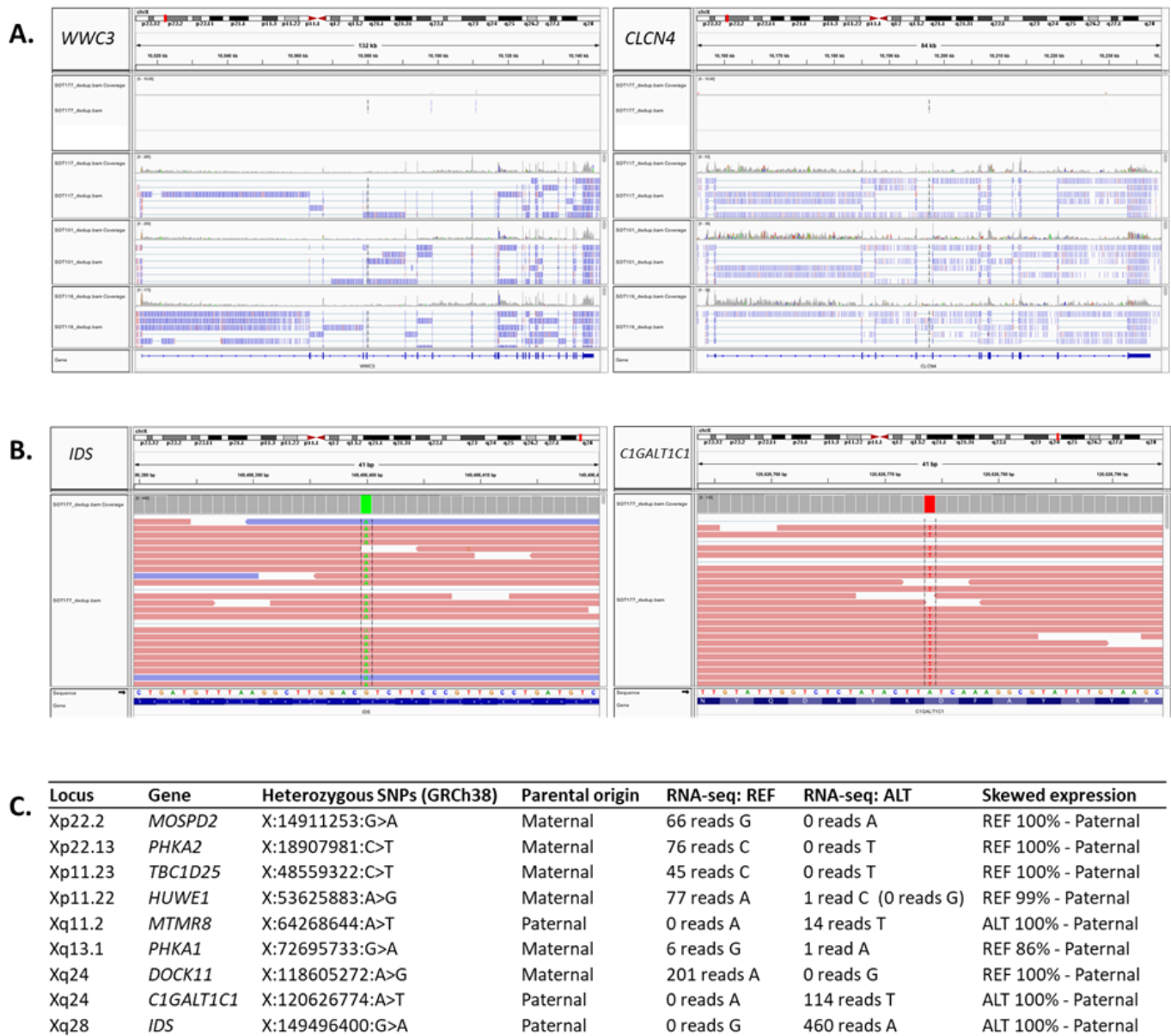
A. *WWC3* ... *CLCN4*

B. *IDS* ... *C1GALT1C1*

C.

Locus	Gene	Heterozygous SNPs (GRCh38)	Parental origin	RNA-seq: REF	RNA-seq: ALT	Skewed expression
Xp22.2	MOSPD2	X:14911253:G>A	Maternal	66 reads G	0 reads A	REF 100% - Paternal
Xp22.13	PHKA2	X:18907981:C>T	Maternal	76 reads C	0 reads T	REF 100% - Paternal
Xp11.23	TBC1D25	X:48559322:C>T	Maternal	45 reads C	0 reads T	REF 100% - Paternal
Xp11.22	HUWE1	X:53625883:A>G	Maternal	77 reads A	1 read C (0 reads G)	REF 99% - Paternal
Xq11.2	MTMR8	X:64268644:A>T	Paternal	0 reads A	14 reads T	ALT 100% - Paternal
Xq13.1	PHKA1	X:72695733:G>A	Maternal	6 reads G	1 read A	REF 86% - Paternal
Xq24	DOCK11	X:118605272:A>G	Maternal	201 reads A	0 reads G	REF 100% - Paternal
Xq24	C1GALT1C1	X:120626774:A>T	Paternal	0 reads A	114 reads T	ALT 100% - Paternal
Xq28	IDS	X:149496400:G>A	Paternal	0 reads G	460 reads A	ALT 100% - Paternal

Figure 6. RNA-seq confirms skewed X-inactivation. **A.** IGV screenshots of RNA-seq data from *WWC3* and *CLCN4*, which lie within the Xp22.33p22.2 deletion. The patient's sample (top track) shows no RNA-seq coverage compared to controls. **B.** IGV screenshots of RNA-seq data for heterozygous SNPs illustrating lack of maternal allele expression. **C**. Table of expression of selected heterozygous X-linked SNPs from across the X chromosome confirming skewing towards the paternal X.